On the consistency of methane ~~isotopologue~~ retrievals using TCCON and multiple spectroscopic databases.

Edward Malina[1], Ben Veihelmann[1], Matthias Buschmann[2], Nicholas M. Deutscher[3], Dietrich G. Feist[4,5,6], and Isamu Morino[7]

[1]Earth and Mission Science Division, ESA/ESTEC, Keplerlaan 1, Noordwijk, the Netherlands.
[2]Institute of Environmental Physics, University of Bremen, Bremen, Germany.
[3]School of Earth, Atmospheric, and Life Sciences, Faculty of Science, Medicine and Health, University of Wollongong NSW 2522 Australia.
[4]Lehrstuhl für Physik der Atmosphäre, Ludwig-Maximilians-Universität München, Munich, Germany.
[5]Deutsches Zentrum für Luft- und Raumfahrt, Institut für Physik der Atmosphäre, Oberpfaffenhofen, Germany.
[6]Max Planck Institute for Biogeochemistry, Jena, Germany.
[7]Satellite Remote Sensing Section and Satellite Observation Center, Center for Global Environmental Research, National Institute for Environmental Studies, Onogawa 15-2, Tsukuba, Japan.

Correspondence: Edward Malina (edward.malina.13@alumni.ucl.ac.uk)

Abstract. The next and current generation of methane retrieving satellites are reliant on the Total Carbon Column Observing Network (TCCON) and other similar systems for validation, and understanding the biases between satellite and TCCON methane retrievals is as important as when TCCON started in ~~2010.~~ 2004. In this study we highlight possible biases between different methane products by assessing the retrievals of the ~~two main methane isotopologues~~ main methane isotopologue $^{12}CH_4$~~and $^{13}CH_4$. For this study we use measurements from two TCCON sites, namely Ascension Island in the Atlantic Ocean and Tsukuba, Japan, with different spectroscopic databases.~~ .

Using the TCCON GGG2014 retrieval environment, retrievals are performed using ~~four~~ five separate spectroscopic databases ~~and a set of spectral fit windows. Databases used~~ from four separate TCCON sites (namely, Ascension Island, Ny-Ålesund, Darwin and Tsukuba). The Spectroscopic databases include the TCCON ~~spectroscopic database~~GGG2014 and GGG2020 spectroscopic databases; the HIgh-resolution TRANsmission molecular absorption database 2016 (HITRAN2016); the Gestion et Etude des Informations Spectroscopiques Atmosphériques ~~2015 (GEISA2015~~2020 (GEISA2020) database; and the ESA Scientific Exploitation of Operational Missions - Improved Atmospheric Spectroscopy ~~Databases~~ (SEOM-IAS) database. We ~~report the biases between the retrievals using standard TCCON methane windows , and specific windows based on the sensitivity of the instruments~~ assess the biases in retrieving methane using the standard TCCON windows and the methane window used by the Sentinel 5-Precursor (S5P) TROPOspheric Ozone Monitoring Instrument (TROPOMI) ~~present on Copernicus Sentinel-5P (S5P) and the future Sentinel 5 (S5) mission present on MetOp-Second Generation satellite. We assess the biases in retrieving methane isotopologues using these different spectral windows and different~~ for each of the different spectroscopic databases. ~~The~~ We further assess the sensitivity of these biases ~~(across windows and databases)~~ to locally changing atmospheric conditions ~~, and uncertainties in the a priori and parameter information, specifically pressure, temperature, methane and water vapour profiles are also quantified~~such as water vapour and temperature.

We find significant biases ~~between retrievalscalculated using differing spectroscopic databases and windows for both methane isotopologues, with up to a 3% bias between $^{12}CH_4$ retrievals. These biases depend on the conditions under which they were captured, with specific windows showing larger biases at higher Solar Zenith Angles (SZA). In addition, the sensitivity to a priori assumptions are shown to be significant and we find the biases between spectroscopic databases change depending on the introduced error, with methane profile shape~~ when compared to standard TCCON retrievals, in some cases up to ~x3 the retrieval noise limit depending on the window and database. We also find strong evidence that different windows in different spectroscopic databases exhibit different levels of sensitivity to changing local conditions such as light path length and water vapour~~profile uncertainty causing significant differences. Retrievals using the~~ . Such that inter-comparisons between different instruments using different retrieval windows should take these sensitivities into account. Based on cross-comparison studies with the standard TCCON methane windows, retrievals using the S5P/TROPOMI spectral range show ~~the results with the least variation between spectroscopic databases, and we~~ results as reliable as the operational TCCON products. We therefore recommend that this ~~band~~ TROPOMI methane window should be considered in future TCCON methane retrievals.

1 Introduction

Methane is widely acknowledged to have a significant impact on the global climate (IPCC, 2014), but the processes via which it enters and is removed from the atmosphere are still ~~not as well understoodas is the case for carbon dioxide;~~ poorly understood, with bottom up (scaled up in-situ measurements) estimations of the global methane budget not agreeing with top down estimations (models) (Kirschke et al., 2013; Saunois et al., 2019). This disconnect is one of many reasons ~~which~~ that has led to the development of multiple satellite missions, with the aim of improving the knowledge of the global methane budget.

The ~~recent~~ launch of the S5P satellite, with the TROPOMI instrument (Veefkind et al., 2012), and the future S5 mission with its Ultra-Violet Near infrared Shortwave infrared (UVNS) instrument (Ingmann et al., 2012), represent a significant advancement in space-based Greenhouse Gas (GHG) remote sensing~~.~~

, building on a decade of progress from the Greenhouse Gases Observing Satellite (GOSAT) (Yoshida et al., 2013). Unlike GOSAT, TROPOMI and UVNS exploit the 4190 – 4340 cm^{-1} spectral range, which has not been explored in detail from previous space-based instruments for methane retrievals. The Scanning Imaging Absorption spectrometer for Atmospheric CartograpHY (SCIAMACHY) (Bovensmann et al., 1999) onboard the ENVIronmental SATellite (ENVISAT) was sensitive to this spectral range, but was plagued with detector issues (ice build-up). The Measurements Of Pollution In The Troposphere (MOPITT) instrument (Drummond and Mand, 1996) is also sensitive to this spectral range, but is also affected by technical issues and has never successfully retrieved methane in this spectral window. The follow-on to GOSAT (GOSAT-2) also uses this spectral range; processing for GOSAT-2 is currently on-going. In addition, the wide spectral sensitivity of the limb viewing Canadian Atmospheric Chemistry Experiment (ACE)- Fourier Transform Spectrometer (FTS) (Bernath et al., 2005) includes

this spectral window, but again the methane products of ACE-FTS do not include retrievals in this window. S5P/TROPOMI and S5/UVNS will therefore be relying on spectroscopic parameters for which only limited experience is available in their application to ~~space based~~ space-based methane retrieval instruments (Checa-Garcia et al., 2015; Galli et al., 2012). ~~This extends to TCCON, which~~ TCCON, although sensitive to this spectral range, has primarily provided its methane abundances retrieved from the 6000 cm^{-1} spectral range, allowing for direct comparisons with SCIAMACHY and GOSAT.

In this study, we make retrievals of the two main methane isotopologues using the TCCON GGG2014 (Toon, 2015) retrieval environment. Spectra are taken from ~~two~~ four different TCCON sites ~~and over multiple seasons,~~ in order to assess the impact of varying atmospheric conditions at different global locations. We assess the differences in abundances of the isotopologues ~~, the retrieval errors~~ and the quality of the fits when retrieved from standard TCCON spectral windows, and methane spectral windows in the TROPOMI/UVNS spectral range. We also quantify the variations in retrieval abundances when using ~~four~~ five separate spectroscopic databases, and the application of non-Voigt line broadening shapes. The sensitivity of the retrievals to ~~errors introduced into the a priori and parameter profiles are assessed~~variations in water vapour concentration and path length are studies, allowing for the assessment of how differing windows and spectroscopic databases are sensitive to these ~~errors~~variations.

TCCON is a global network of 27 ground based Fourier Transform Spectrometers (FTS) (Wunch et al., 2010), with the primary aim of providing reference total column (an weighted average value for a nadir viewing profile) abundances of numerous atmospheric species calibrated against aircraft profiles (Wunch et al., 2010, 2011), including methane, for validation and cross-calibration purposes. TCCON operates in a wide spectral range (4000 – ~~15000~~ 11000 cm^{-1}) and records direct solar spectra. TCCON is currently one of the key sources of reference data for the validation of satellite-based GHG retrievals~~(Yoshida et al., 2011; Crisp et al., 2012; Parker et al., 2015).Examples include~~ , e.g. the Orbiting Carbon Observatory (OCO)-2~~and the Greenhouse Gases Observing Satellite (GOSAT) (Kuze et al., 2009)~~, GOSAT and TROPOMI (Yoshida et al., 2011; Crisp . TCCON instruments have both high spectral resolution (0.02 cm^{-1}), and high Signal to Noise Ratios (SNR) due to direct solar viewing geometry, and insensitivity to atmospheric scattering, thus making TCCON measurements higher quality than satellite measurements ~~.~~ and excellent comparison datasets for satellite retrievals.

TCCON and TROPOMI/UVNS both have overlapping spectral windows in the Shortwave Infrared (SWIR) methane absorption regions, highlighted in Table 1.

Table 1. Methane SWIR windows commonality between S5P/S5 and TCCON

Methane window	S5P/TROPOMI	S5/UVNS	TCCON
5970-6289 cm^{-1}	N	Y	Y
4190-4340 cm^{-1}	Y	Y	Y

When validating methane products from TROPOMI and UVNS, retrieval products using the 4190 – 4340 cm^{-1} window ~~,~~will be compared with TCCON methane products ~~generating~~ generated using the standard TCCON windows (Table~~2~~ 4). Therefore potential biases associated with the choice of fit windows ~~needs to~~ should be quantified and understood. Indeed, if the 4190 –

4340 cm^{-1} window proves to be ~~accurate/stable~~as accurate as the standard TCCON windows, then there is justification to integrate TCCON retrievals from this window into future TCCON retrieval products. ~~Numerous~~ In addition, numerous algorithms will be used to provide methane data products from TROPOMI/UVNS (Hu et al., 2016; Schneising et al., 2019), ~~all of which will~~ which may use differing spectroscopic databases and are therefore subject to differing biases. ~~The~~ Building on examples of similar past studies (Checa-Garcia et al., 2015; Galli et al., 2012), the high SNR and high spectral resolution makes TCCON data an excellent resource to ~~perform retrievals of methane isotopologues, and~~ assess any potential variations due to differences in the spectroscopic databases~~, building on examples of similar past studies (Checa-Garcia et al., 2015; Galli et al., 2012)~~. By investigating the biases present in TCCON observations made at several sites ~~, we~~ over several seasons. We can infer some of the potential spectroscopic related biases in satellite retrievals, and their dependencies on ~~temperature and pressure. Our findings will inform as to the potential source of biases and~~ local conditions such as water vapour that are relevant to ongoing TROPOMI validation, and future S5/UVNS validation. ~~We also make recommendations on spectral windows and databases for future methane retrievals.~~

~~TCCON methane products are the result of a standardised process where a weighted average of three retrieved values from three TCCON fit windows (described in Table 2 below) is reported. Assessments of the biases present in between these windows, with respect to the spectroscopic databases may help inform the future of TCCON methane products.~~

In addition to assessing the window and spectroscopic source biases for the ~~two~~ main methane isotopologues, the opportunity is taken to calculate the $\delta^{13}C$ metric ~~which is a ratio of these isopologues~~ (see Eq~~. 2~~ 2). This is a metric ~~which~~ that has been used in numerous studies globally to differentiate methane source types (Fisher et al., 2017; Nisbet et al., 2016; Rigby et al., 2017; Rella et al., 2015), e.g. ~~industrial~~ fossil fuel burning or wetlands. Calculating total column values of this metric would be highly beneficial for understanding the global methane budget, but is unlikely to be achievable with TCCON with an accuracy that would be sufficient for that purpose. However, calculation of $\delta^{13}C$ with TCCON will allow for an assessment of how far current technology is from making a useful total column assessment. ~~Calculation of the~~ $\delta^{13}C$ metric requires the concentration of the two main methane isotopologues $^{12}CH_4$ and $^{13}CH_4$, which make up roughly ~~98~~99% and 1.1% of global atmospheric methane respectively. Almost all measurements of this metric are limited to in situ studies or airborne flask measurements, which although highly accurate, by their nature are spatially limited. Some effort has gone into satellite based retrievals of this metric (Buzan et al., 2016; Weidmann et al., 2017; Malina et al., 2018, 2019), but the results of these studies show this to be a challenging task. Therefore the calculation of the $\delta^{13}C$ metric is a target of secondary importance in this study.

This paper is structured as follows, section 2 outlines the methods used in this study, including details about the TCCON sites and spectra used, as well as the retrieval method. Information about the spectroscopic databases used in this study are also given. The results of this study are shown in section ~~3. Section 4 outlines~~ 3 outlining the biases between sites and databases, including an assessment of the sensitivity of the retrievals to ~~introduced errors in the a priori data and~~ local condition variability. Section ~~5~~ 4 discusses the results shown in sections 3~~and 4~~, and conclusions are shown in section ~~6.~~ 5.

2 Methods, tools, datasets and requirements

2.1 TCCON ~~spectra and tools~~sites used in study

We use TCCON spectra from ~~two different sites , firstly the Ascension Island site, found in the middle of the Atlantic Ocean near the equator. The second site is the Tsukuba site, near Tokyo in Japan, and at a higher latitude than Ascension Island. Ascension Island has an arid climate with a little precipitation , which remains largely constant through the year and does not have designated seasons but is~~ four different sites identified in Table 2. Datasets over a single year were chosen in order to represent a wide range of seasonal conditions. The years chosen represent the years with maximum data coverage.

Table 2. TCCON sites used in this study.

TCCON Site	Lat/Lon	Date Range	Number of Spectra	Conditions
Ascension Island, Atlantic ocean	7.92°S, 14.3°E	Jan-Dec 2015	1518	Arid, little precipitation subject to some ~~variation. Tsukuba is subject to seasonal effects, with hot wet summers and~~ seasonal variation.
Darwin, Australia	12.5°S, 130.9°E	Jan-Dec 2020	39160	Tropical, significant water vapour background.
Ny-Ålesund, Spitsbergen	78.9°N, 11.9°E	April-Oct 2019	6315	Cold, dry, limited short-term variability.
Tsukuba, Japan	36.1°N, 140.1°E	Jan-Dec 2020	6162	Seasonal, cold dry winters, ~~these two sites represent a wide range of atmospheric conditions. The Tsukuba spectra are generally captured in a narrow spread of SZAs, typically 35°<SZA <60°; Ascension Island spectra are captured under a much wider range of SZA, typically 10°<SZA<90°. This means that there will be larger variations in SNR for Ascension Island than Tsukuba,~~

The mean background conditions for each site, as well as the variations over the dataset periods shown in Table 2 are indicated in Table 3. Significant variations in conditions and SZA are apparent between the TCCON sites, suggesting a wide range of capture conditions. We note the distributions of the conditions shown in Table 3 may not be normally distributed, but these statistics serve as a useful baseline to show the condition variations between the sites.

Table 3. TCCON sites water vapour, temperature and SZA average and variation.

TCCON Site	Water Vapour mean $\pm\sigma$	Temp mean $\pm\sigma$	SZA mean $\pm\sigma$
Ascension Island	4510 ppmv $\pm$ 890	27.5 °$\pm$ 1	38°$\pm$ 18
Darwin, Australia	5430 ppmv $\pm$ 1740	30.9°$\pm$ 3	45°$\pm$ 18
Ny-Ålesund, Spitsbergen	1440 ppmv $\pm$ 600	1.7°$\pm$ 6	69°$\pm$ 8
Tsukuba, Japan	3200 ppmv $\pm$ 2470	22.9°$\pm$ 9	50°$\pm$ 18

2.2 GFIT Retrieval Algorithm

In this study we use the GGG2014 environment, which includes the GFIT retrieval algorithm (Wunch et al., 2010), ~~the standard algorithm used by the TCCON sites for processing and distributing trace gas column abundances. GFIT~~ which is summarised briefly here~~;~~ . GFIT employs a nonlinear least-squares fitting scheme~~.~~ : A forward model (radiative transfer model which simulates radiation transfer through an atmosphere or a body of gas) is used to calculate synthetic irradiance spectra based on a set of parameters known as state vector elements (typically trace gas concentrations) and model parameters (e.g. temperature and pressure profiles). ~~This~~ These synthetic irradiance spectra ~~is~~ are then fit to the measured irradiance ~~spectrum~~ spectra by adjusting the state vector elements to provide a final result, normally a trace gas abundance. In the case of GFIT the state vector ~~includes~~ can include the following.

- first target gas scaling factor (desired output).
- interfering gas scaling factor.
- continuum level of the irradiance spectrum.
- continuum tilt
- continuum curvature
- frequency shift
- zero level offset
- solar scaling (differences in shifts of atmospheric and solar lines)

– fit channel fringes

Note that not all of the above are not routinely included in the state vector, for example the continuum curvature especially is not commonly included in the state vector. This option is designed to remove instrument features, but may also attempt to remove other effects due to the spectroscopic database, as noted in the TCCON wiki (TCCON, 2020). GFIT assumes a fixed profile shape for each trace gas, and the sub-column ~~amount~~ amounts for each altitude/pressure level are not independently scaled. Unlike in most satellite retrieval algorithms, aerosol and albedo terms are not included in the state vector, ~~this is~~ because TCCON operates in direct solar viewing, where scattering is considered unimportant and surface terms are not necessary. The retrieved trace gas column is calculated by multiplying scaling factors from the retrieved state vector by the a priori vertical column abundances. Dry air Mole Fractions (DMF) are calculated by dividing the scaled trace gas column with the total column O_2, retrieved from a wide window in the 7885 cm^{-1} spectral range multiplied by the volume mixing ratio of O_2 0.2095. DMF gas ~~concentrations identify retrieved concentration~~ volumes identify retrieved abundances as mole fractions, as opposed to absolute concentrations, all retrieved $^{12}CH_4$ ~~and $^{13}CH_4$ concentrations~~ abundances are referred to as DMF values.

Because of the high spectral resolution of the TCCON instruments (0.02 cm^{-1}), most spectral lines are resolved, radiative transfer calculations are performed on a line-by-line basis. GGG includes a spectroscopic database in its environment, which is similar to other more widely adopted databases (see below). TCCON has a standard set of spectral windows for methane retrievals, all of which are in the 6000 cm^{-1} methane absorption window range. In this study we include the TROPOMI/UVNS SWIR spectral windows (4190-4340 cm^{-1}). This window along with a description of all of the windows considered in this study are described in Table~~2~~ 4 below.

Table 4. Spectral windows used in study.

Window
1
2
3
4
~~5 4190-4340 $^{13}CH_4$ $^{12}CH_4$, CO_2, H_2O, HDO, CO, HF, N_2O, O_3 Sentinel 5 baseline 6 6007-6145 $^{13}CH_4$ $^{12}CH_4$, CO_2, H_2O, N_2O, HDO~~

Windows 2-4 are standard TCCON methane retrieval windows which in this study are used for $^{12}CH_4$, and ~~windows~~ window 1 is based on the TROPOMI spectral window (Galli et al., 2012; Hu et al., 2016), given that no standard windows exist in this spectral window for TCCON. ~~Windows 5~~ In addition, TCCON methane products are the result of a standardised process where a weighted average of three retrieved values from windows 2, 3 and ~~6 are repeats of windows 1 and~~ 4 ~~, but with $^{13}CH_4$ as the target~~described in Table 4.

2.2.1 ~~Spectroscopic Databases~~

~~The introduction of~~ For $^{13}CH_4$ ~~into spectroscopic databases in the TROPOMI spectral region is relatively recent, and in the case of HITRAN, was only introduced in the 2012 release. Indeed Gordon et al. (2017) reports that numerous new $^{13}CH_4$ lines were introduced into the latest HITRAN2016 release, this implies that the spectroscopic parameters of $^{13}CH_4$ in this region is not yet settled. A review of the documents released with numerous spectroscopic databases (Gordon et al., 2017; Jacquinet-Husson et al., 2016; Bi suggest that $^{13}CH_4$ lines are not all sourced from the same laboratory studies. We therefore decided to compare methane isotopologue retrieval from four~~ retrievals, windows 1 and 4 are used.

2.3 Spectroscopic Databases

We use parameters from five separate spectroscopic databases, which are as follows: 1) ~~the~~ The database included with GGG2014 (Toon, 2015), which currently assumes a Voigt line shape for all lines. 2) The database included with the updated GGG2020 software, referred to in this study as GGG2020, which includes numerous updates to the GGG2014 spectroscopic parameters, and some application of non-Voigt parameters. 3) HITRAN2016, ~~HITRAN~~ which is a well-established spectroscopic database that has been used in numerous satellite based studies previously (Galli et al., 2012). ~~The~~ Methane has been updated in the current release HITRAN2016 (Gordon et al., 2017) ~~has been revised~~ from the previous release (HITRAN2012)~~in terms of methane~~, with new lines and parameters included for both of the main isotopologues. HITRAN2016 ~~does include~~ includes the additional parameters required to model non-Voigt lines shapes, however the current version does not include these parameters for methane (at the time of writing). ~~3) The GEISA2015 database (Jacquinet-Husson et al., 2016)~~ 4) The GEISA2020 database (Delahaye et al., 2021) is another spectroscopic database, similar in design and goals to the HITRAN databases. The GEISA database does not currently include non-Voigt line shape parameters. ~~4~~5) SEOM-IAS (Birk et al., 2017), specifically developed for the TROPOMI spectral window and designed around non-Voigt atmospheric line shape profiles. This database only has data within the 4190-4340 cm^{-1} spectral range, and can therefore only contribute to ~~windows~~ window 1 ~~and 5~~ of this study.

For clarification purposes, there are no official releases of the spectroscopic parameters used in the GGG TCCON retrievals. We refer to the databases used in this study as GGG2014 and GGG2020 in order to differentiate with them, based on the GGG retrieval environment releases, with GGG2020 due for release in the near future (Laughner et al., 2021).

Some work has been performed previously comparing spectroscopic databases e.g. (Jacquinet-Husson et al., 2016; Armante et al., 2016), ~~but~~ generally indicating that the need to resolve differences between spectroscopic databases remains. Yet none have specifically targeted the TROPOMI SWIR spectral region, therefore this study is the first case with respect to the TROPOMI spectral window with TCCON.

2.3.1 ~~Voigt vs non-Voigt line shape profiles~~

~~Ngo et al. (2013) states that~~ Further to exploring the impact of differing spectroscopic database parameters, we investigate the use of non-Voigt broadening parameters. Ngo et al. (2013) find the standard Voigt profiles used for spectral line broadening may be inadequate for trace gas retrievals (based on laboratory studies), which can lead to errors larger than instrument precision requirements. In order to calculate more accurate line shapes for remote sensing purposes, numerous models have been

proposed. In this paper we use the quadratic Speed Dependent Hard Collision (qSDHC) model (Ngo et al., 2013; Tran et al., 2013). This model includes additional parameters based on speed dependence of collisional broadening and velocity changes of molecules due to collisions, on top of the standard parameters of pressure-induced air broadening, and pressure induced line shift. Note that only the SEOM-IAS database ~~use~~ uses these additional parameters, the remaining spectroscopic databases do not include these parameters for methane at the time of this paper. We use the FORTRAN routines provided with Ngo et al. (2013) to implement the qSDHC model into the GFIT algorithm, modified to include first order Rosenkranz line mixing effects. Mendonca et al. (2017) report that incorporating speed dependent and line mixing has a significant effect on calculated methane columns when compared against assuming Voigt dependency. They find a 1.1% difference in total methane column abundances from 131,124 spectra. The implication ~~being~~ is that it is important to account for the additional physical parameters included in non-Voigt models, when retrieving methane.

2.4 ~~Metrics~~

We note the introduction of $^{13}CH_4$ into spectroscopic databases in the TROPOMI spectral region is relatively recent, and in the case of HITRAN, was only introduced in the 2012 release (Brown et al., 2013), thus suggesting that $^{13}CH_4$ spectroscopic parameters may retain high levels of uncertainty.

~~Our main assessment metrics~~

2.4 Analysis structure and metrics

The following section describes the assessment metrics used in this study~~are as follows.~~

~~Averaging Kernels (AK): the AKs capture the sensitivity of the retrieved state vector to the truth, and is defined as $\mathbf{A} = \partial\hat{\mathbf{x}}/\partial\mathbf{x}$, where $\hat{\mathbf{x}}$ is the retrieved state vector and $\mathbf{x}$ is the truth. AKs are typically used in satellite and ground-based remote sensing to characterise the vertical sensitivity profile of a retrieval.~~

~~Transmission spectra.~~ . Firstly we assess the quality of the fit of the measured and modelled spectra for each window indicated in Table 4 for each spectroscopic database at each TCCON site. The quality of the fit is expressed through Root Mean Square Error (RMSE) of the residual between the calculated transmission spectra, and the TCCON measurement transmission spectra, ~~expressed as the RMSE. The quality of the fit, expressed via the~~ and the χ^2 test, quantitatively defined as:

$$\chi^2 = \sum_i [\mathbf{y_{measured}} - \mathbf{y_{calculated}}]^2. \quad (1)$$

.

Where $\mathbf{y_{measured}}$ refers to the measured TCCON spectrum, and $\mathbf{y_{calculated}}$ is the synthetic spectrum calculated by the forward model.

~~Retrieved values. Standard deviation of the DMF~~ Secondly we assess the variance of the calculated DMFs of $^{12}CH_4$ for each window~~(σ_{window}).Standard deviation of the DMF between all windows~~ , spectroscopic database and TCCON site w.r.t the standard methane window used in TCCON retrievals currently, which is a weighted average of windows 2, 3 and 4. This variance is described through the RMSE of the residual between the retrieved DMF of $^{12}CH_4$ for a specific ~~database~~

($\sigma_{inter-window}$)Bias of the retrieved mean of the DMF for each window against the retrieved mean of the equivalent window using the TCCON spectroscopic database, which is taken as the reference in the present study due to its pedigree in validations for satellite missions. window and the retrieved DMF of the standard TCCON retrieval window, normalised by dividing by the retrieval error of the standard TCCON retrieval window (NRMSE). The variance is also given by the absolute mean residual between the retrieved DMF of $^{12}CH_4$ for a specific window and the retrieved DMF of the standard TCCON retrieval window, normalised by dividing by the retrieval error of the standard TCCON retrieval window (NAmean).

A posteriori error Total uncertainty in the retrieved abundances of the methane isotopologues, including systematic and random errors. Wunch et al. (2010) states that systematic errors typically dominate for TCCON retrievalsFollowing the assessment of the retrieval variance between windows and databases, we investigate if locally changing conditions impact biases between spectroscopic databases and windows. Variations in the retrieval conditions throughout the course of a day of measurements are included in TCCON error budgets, for example artefacts can appear in TCCON retrievals at extreme SZA values (Wunch et al., 2011) .

δ^{13}C: Methane isotopologues abundances are typically expressed in the form of the following metric.

$$\delta^{13}C = \left(\frac{(^{13}CH_4/^{12}CH_4)_{sample}}{(^{13}CH_4/^{12}CH_4)_{VPDB}} - 1 \right) \times 1000‰,$$

where VPDB refers to Vienna Pee Dee Belemnite, an international reference standard for 13C assessment. Tropospheric methane typically exhibits a δ^{13}C value of roughly -47‰ (Rigby et al., 2017), and total column measurements from TCCON are unlikely to deviate from this value to a significant degree. Therefore this tropospheric δ^{13}C value acts as a useful proxy, to determine the stability and variability associated with retrievals of methane isotopologues from different spectral windows, spectroscopic databases, location and time using the tropospheric δ^{13}C value as a baseline.

In an ideal scenario we would compare our results with some reference results, however we are currently unaware of total column $^{13}CH_4$ retrieval data. We therefore perform our comparisons with respect to the TCCON spectroscopic database, under the assumption that biases are already present, which can be assessed at a later date if there is benefit to doing soWe therefore investigate if the methane retrieval biases vary with respect to the following local parameters 1) SZA, where extreme angles can cause errors in the air-mass assumptions and affect characteristics of the Instrument Lineshape function (ILS) (Wunch et al., 2011). 2) Water vapour (retrieved by TCCON) through the course of a day at a range of TCCON sites. The GFIT retrieval algorithm is a scaling retrieval algorithm for all trace gas fitting, meaning that an incorrect apriori trace gas profile shape will yield errors in the retrieval. The GFIT water vapour apriori is based on a profile taken at midday for each specific retrieval, meaning that any significant variations from this daily profile will yield errors in the retrieval, that will vary depending on the impact of water vapour on a specific spectral window. 3) Temperature, which is not included in the retrieval state vector and dependencies on temperature will not be removed in the retrieval process. Temperature errors are introduced through the spectroscopic cross sections (An et al., 2011), therefore poor knowledge of spectroscopic parameters will potentially lead to temperature based errors.

2.5 ~~Analysis criteria~~

These dependencies are quantified by identifying the possible existence of a linear correlation (using Pearson correlation coefficient and linear fit gradient) between the variations of water vapour, SZA and measured temperature against the bias between the retrieved methane isotopologue DMFs for each window and spectroscopic database, against the DMFs from the standard TCCON methane retrieval window normalised by the noise from the standard TCCON methane retrieval window.

~~There are two aspects to this study, the primary aspect is an assessment of the biases between spectral windows and spectroscopic databases w.r.t the two main methane isotpologues. TCCON~~ The magnitude of the metrics defined above can be put into context by comparisons with the TCCON error budget. TCCON typically aims for precision of <0.3% on methane retrievals, and has a rough estimate of 1% systematic uncertainties (dominated by in-situ calibration which ~~vary depending on site~~ can affect sites differently (Wunch et al., 2015)). Therefore it is possible to judge the ~~variations of the~~ variation of $^{12}CH_4$ DMFs between windows and databases based on these biases and ~~precisions. In order to judge inter-window/spectroscopic database biases, we often compare the relative difference of the retrievals with respect to window 4 of the TCCON spectral database, henceforth described as the 'reference value'. We choose this window because it is the most commonly used in space based retrievals at this time (e.g. GOSAT), and the TCCON spectral database as it is the most established with TCCON retrievals. The relative difference is calculated as the difference between the retrieval and the reference value, divided by the reference value. This assessment is shown in Fig. 3.~~ precision.

~~In terms of~~ Finally, although the quality of the $^{13}CH_4$ ~~, there are no published precision and accuracy requirements or statistics with~~ fit metrics in this study are not covered in detail, we instead calculate the $\delta^{13}C$ metric in order to understand the plausibility and variation of retrieving $^{13}CH_4$ from TCCON. Fundamentally the final aim of retrieving $^{13}CH_4$ is to calculate $\delta^{13}C$. ~~$\delta^{13}C$ has been used to differentiate between methane source types (Fisher et al., 2017; Nisbet et al., 2016; Rigby et al., 2017; Rella et , and variations of this value has been linked with variations in the global methane budget (Rigby et al., 2017; Menorton et al., 2016) .~~ How much $\delta^{13}C$ varies in the total varies in the total column is a complex issue (Weidmann et al., 2017; Malina et al., 2018, 2019), in-situ studies (Nisbet et al., 2016; Rigby et al., 2017; Fisher et al., 2017) all show that an uncertainty of «1‰ in $\delta^{13}C$ is required in order to determine natural annual variability at the surface. However, variability in $\delta^{13}C$ can be higher in the troposphere and stratosphere due to variability of the OH sink and the fractionation caused by OH (Röckmann et al., 2011; Buzan et al., 2016), with evidence that $\delta^{13}C$ can vary by up to 10‰ in different air parcels (Röckmann et al., 2011). Based on these ~~factor~~factors, we assume a rough total column $\delta^{13}C$ variability of 1‰, which equates to a total uncertainty of <0.02 ppb on $^{13}CH_4$ retrievals, or roughly 0.1% of the total column. This is clearly an unrealistic target for individual retrievals, given the uncertainty requirements for $^{12}CH_4$ described above. Nevertheless precision errors will be low due to the nature of TCCON, and through the fact that TCCON sites are situated in a fixed position, allowing for long term averaging to reach a required precision target. Therefore one of the minor aims of this study is to identify how far away TCCON uncertainty (including systematic errors) is from the desired uncertainty of <1‰ $\delta^{13}C$.

2.5 ~~Sensitivity analysis~~

$$\delta^{13}C = \left(\frac{(^{13}CH_4/^{12}CH_4)_{sample}}{(^{13}CH_4/^{12}CH_4)_{VPDB}} - 1 \right) \times 1000‰, \quad (2)$$

~~In addition to understanding any biases that may exist between spectroscopic databases and windows under nominal conditions, it is important to assess if these biases vary with respect to errors or assumptions in retrieval conditions, this type of assessment is known as a sensitivity analysis (Wunch et al., 2011; Hu et al., 2016). In this study we assess the impact of two key error sources, firstly how changing retrieval conditions over a series of TCCON measurements can affect biases, and secondly if uncertainty on the input retrieval information can impact bias magnitudes~~where VPDB refers to Vienna Pee Dee Belemnite, an international reference standard for ^{13}C assessment. Tropospheric methane typically exhibits a δ^{13}C value of roughly -47‰ (Rigby et al., 2017), and total column measurements from TCCON should not deviate from this value to a significant degree. Therefore this tropospheric δ^{13}C value acts as a useful proxy, to determine the stability and variability associated with retrievals of methane isotopologues from different spectral windows, spectroscopic databases, location and time using the tropospheric δ^{13}C value as a baseline. In terms of $^{13}CH_4$, there are no published precision and accuracy requirements or statistics with TCCON.

2.4.1 ~~Local condition variations~~

3 Results

~~Variations in~~

3.1 Quality of spectral fitting

An example of residual transmission spectra from the Ny-Ålesund site is shown in Fig 1, with the standard deviation of a selection of retrievals within the same time period indicated by the ~~retrieval conditions throughout the course of a day of measurements are included in TCCON error budgets, for example artefacts can appear in TCCON retrievals at extreme SZA values (Wunch et al., 2011). We therefore investigate if the methane retrieval biases vary with respect to SZA and water vapour (retrieved by TCCON) changes through the course of a day at both TCCON sites. These dependencies are quantified by identifying the possible existence of a linear correlation (coefficient of determination) between the variations of water vapour and SZA against the bias of the retrieved methane isotopologue DMFs for each window and spectroscopic database, against the DMFs from window 4 from the TCCON spectroscopic database (otherwise known as the 'reference value')~~red lines. Qualitatively we note clear differences in the quality of the fits between windows and databases, for example there are clear deviations apparent, especially in window 1 for HITRAN and GEISA.

3.1.1 ~~A Priori and parameter errors~~

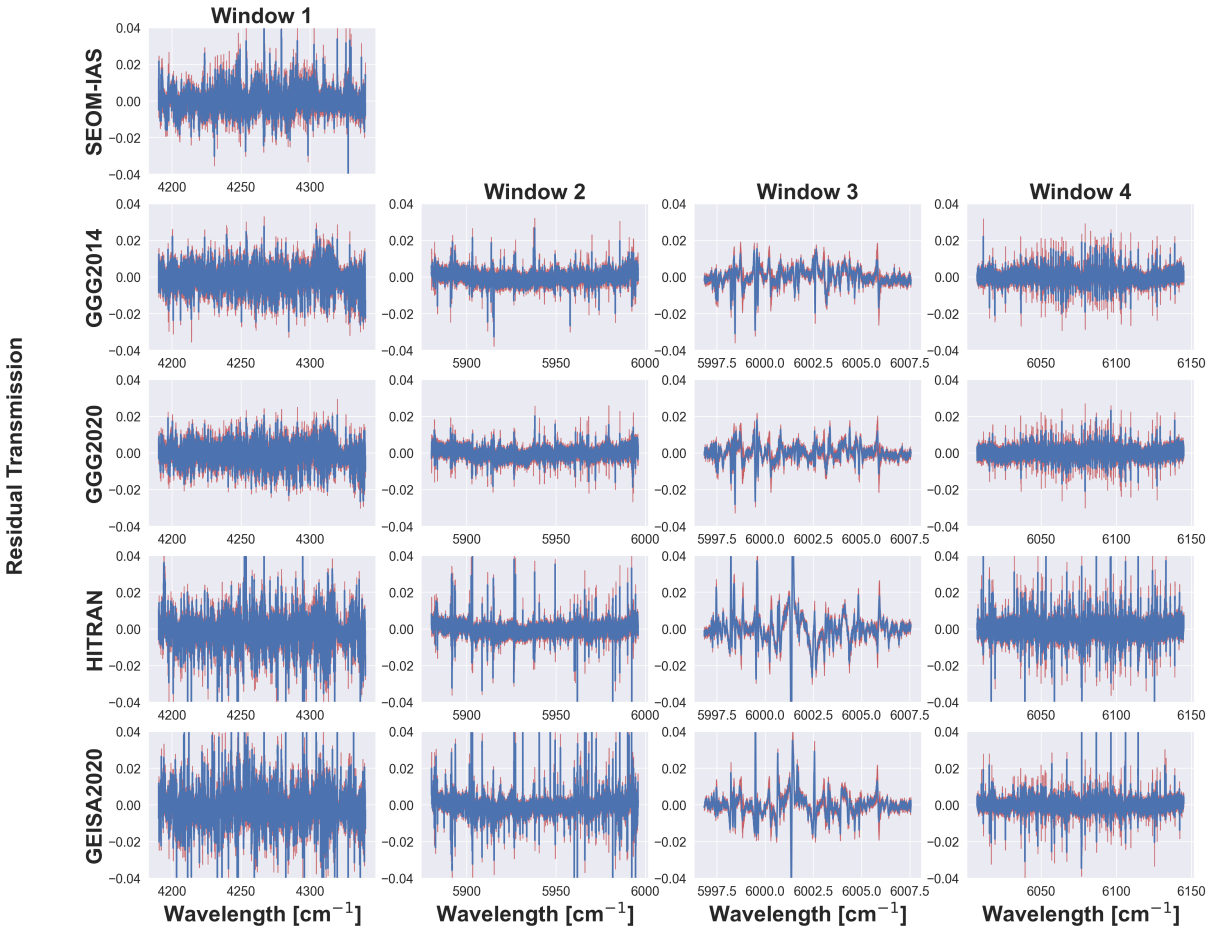

Figure 1. Example residual transmission spectra calculated from measured and fitted spectra from the Ny-Ålesund in 2019. The blue line indicates an example of the fit residual between the calculated transmission and the measured transmission. The red lines indicates the standard deviation of the residual, based on all spectra taken over the entire dataset. The columns of this figure identify the residuals of a specific window, and the rows a specific database, as identified in the axis labels.

~~An important aspect of all trace gas retrievals are the sensitivities to uncertainties in the input a priori and parameter profile information. A priori information refers to quantities which are estimated as a part of the retrieval process (such as trace gases), and parameters refers to quantities necessary for retrieval, but are not estimated as a part of the retrieval process (such as temperature) (Rodgers, 2000). Here we investigate how the retrieved isotopologue DMFs vary between spectroscopic databases and windows when errors are applied to the a priori and parameter information. These profiles are derived from different models which carry inherent uncertainty e. g. (Wunch et al., 2011; Rahpoe et al., 2013), this can be assessed by perturbing the input parameter profiles and comparing the output results.~~ The analysis statistics for the residual transmission spectra (as discussed

in sect. 2.4) shown in Fig 1 are shown in Fig 2, as well as the associated statistics for the other TCCON sites considered in this study. What is clear from Fig 2 is the fit statistics for each spectroscopic database, irrespective of TCCON site and window generally have the same pattern in terms of quality. For window 1 SEOM-IAS usually has the best fit metrics (i.e. the lowest magnitudes), followed by GGG2020, GGG2014, HITRAN and then GEISA. In windows 2-4 where SEOM-IAS has no data, GGG2020 typically shows the highest quality fits, suggesting the latest iteration of the GGG2020 spectroscopic parameters has superior performance to the older version.

~~The a priori and parameter atmospheric datafor the GFIT algorithm is based on two sources; the pressure, temperature and humidity data are drawn from the National Centers for Environmental Prediction (NCEP)/National Center for Atmospheric Research models (NCAR). The trace gas profiles are built from empirical models developed from a combination of data from atmospheric balloon borne sensors, and from the satellite instrument ACE-FTS (Wunch et al., 2010, 2011). We investigate the sensitivities of the retrievals to the following input parameter uncertainties~~Window 1 typically shows the poorest fit metrics of all windows, possibly because it is the largest window, but also because it is more complex region in terms of absorption (Brown et al., 2013) than the other windows. Window 4 for example is also wide, but typically shows higher quality fits than any of the other windows in this study. The implication being that the knowledge of spectroscopic parameters in window 1 is still lacking in comparison to the traditional TCCON windows. There are differences in the metrics between TCCON sites, with Ascension Island showing poorer fits than any of the other sites, similar to Darwin. This is to be expected however since these instruments are not identical, and capture spectra under differing conditions. We note that all instruments are run according to TCCON specifications but their respective configurations are not exactly the same. This is normal and necessary as different sites need local adjustments to account for different local conditions such as altitude, humidity or cloud conditions. Most of the effects caused by such individual configurations are removed by the differential CO_2 and CH_4 DMF retrievals but will affect individual spectra. For example, in the case of Tsukuba and Ascension, the configuration effects cannot be compared directly except for detector noise, which turned out to be comparable. However, the signal on the detector of the Ascension Island instrument is at least 50% lower than that of the Tsukuba instrument.

~~A priori and parameter error magnitude. Error Source Magnitude Methane profile shift 2% Methane profile shape Swap seasonal profiles Water vapour profile shift~~ Likely reasons are: 1) The Ascension FTS runs on a higher spectral resolution (0.014 cm^{-1} vs. 0.02 cm^{-1}) and a faster scanner speed (10 ~~% Pressure profile shift~~ kHz vs. 7.5 kHz). Both reduce integration time per spectral pixel. 2~~% Temperature profile shift 2 K~~

~~The magnitudes identified in Table 3 mirror those used in a similar study focused on S5P/TROPOMI (Hu et al., 2016), given that S5P/TROPOMI validation is one of the focus points of this study. Since methane is the gas under investigation in this study, it is important to understand how shifting the input atmospheric profile affects the output. Since GFIT is a scalar retrieval algorithm, retrievals using an incorrect methane profile (e. g. tropopause in the incorrect layer) could induce biases which vary between windowsand spectroscopic databases. Therefore the April and July Tsukuba methane profiles are swapped, and the August and October Ascension Island profiles are swapped to induce errors. Water vapour is the main interfering trace gas in these windows, and uncertainties in the starting knowledge of water vapour may yield different results from different windows or spectroscopic databases. GFIT directly retrieves methane and water vapour, but pressure and temperature are not~~

included in the state vector and are not retrieved, meaning dependencies on pressure and temperature will not be removed in the retrieval process. Pressure column uncertainties can affect methane retrievals in two ways. The first is through the retrieval of O_2 which is used to convert the total column concentration of methane into DMFs, the second is through pressure dependence of spectroscopic absorption. For temperature, errors areintroduced through the spectroscopic cross sections, Eq (3) describes the temperature dependency of the line intensity (An et al., 2011).

$$\frac{S(T)}{S(T_0)} = \frac{Q(T_0)}{Q(T)} exp(-\frac{hcE_0}{k}(\frac{1}{T} - \frac{1}{T_0})),$$

where $S(T)$ is the line intensity at temperature T, $Q(T)$ is the total partition function of the absorbing molecule at temperature T, $S(T_0)$) The illumination of the InGaAs detector on Ascension is kept low on purpose to avoid saturation. This setting cannot be readjusted in between site visits and has to last for months. Other sites may use similar techniques, and $Q(T_0)$ are as before but at temperature T_0, E_0 is the lower state energy, and h, c and k are constants. Equation (may vary depending upon need. 3) suggests that if there are significant differences between the spectroscopic databases, most notably in the lower state energy level, then the temperature and pressure dependency uncertainty of the retrievals will vary depending on the database. Thus implying that the bias between spectroscopic databases can vary depending on spatial and temporal conditions. The solar tracker has known issues with pointing at the centre of the sun at low SZAs but cannot be replaced easily. In addition, dust buildup on the solar tracker mirrors reduces the reflectively of the mirrors quickly. They are cleaned weekly but a signal loss in the order of 20% over a few days is not uncommon.

To quantify the impact of these introduced errors we use two methods. Firstly the metrics described in sect 2.2 for 'retrieved values' are used for retrievals from April 2016 from the Tsukuba site, allowing for a direct comparison between the 'nominal cases' and the 'perturbed' sensitivity analysis cases. Secondly we use linear regression to compare the retrieved DMFs of [12]

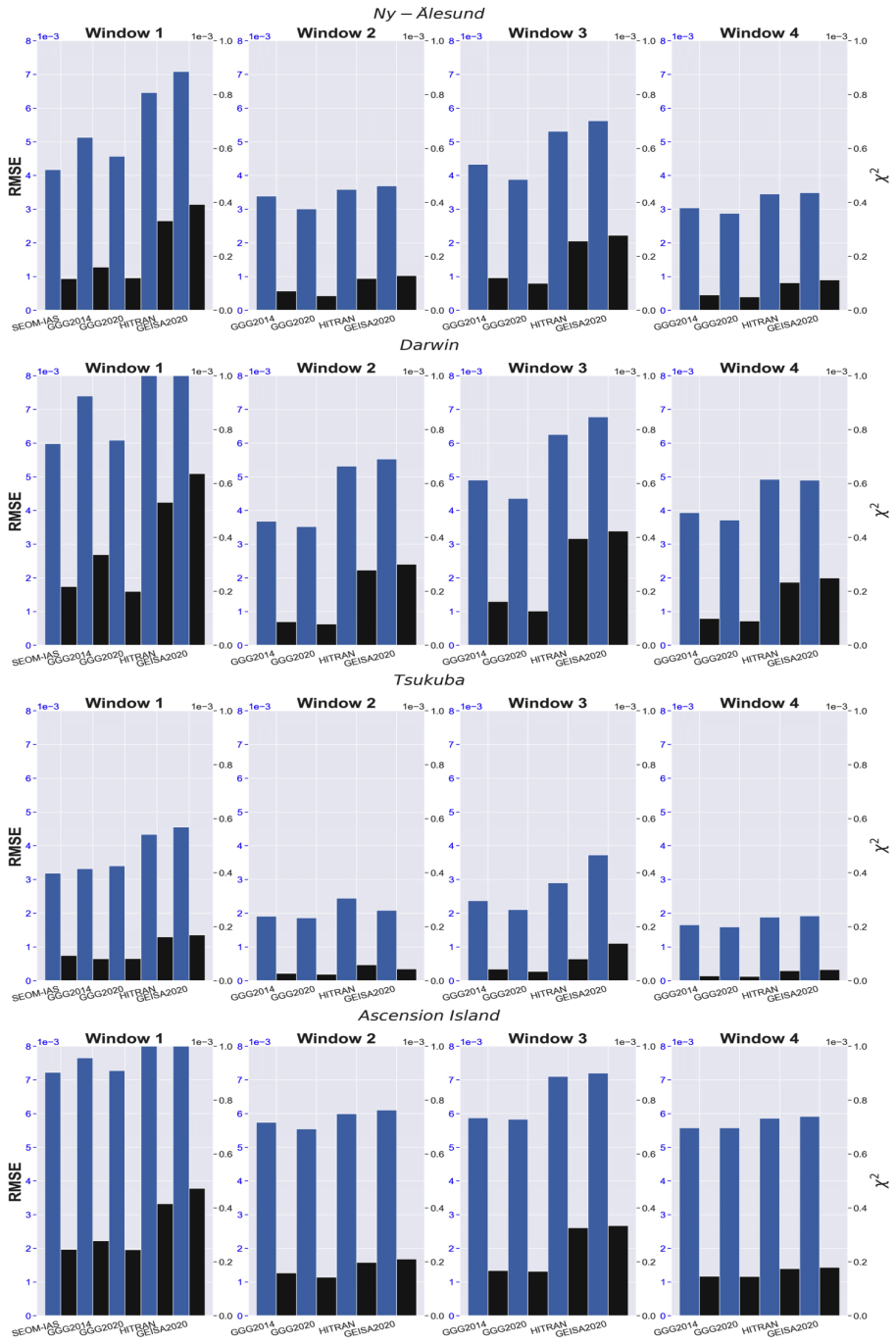

Figure 2. Bar chart indicating the fit statistics for a selection of retrievals from each of the TCCON site. Each row of the figure refers to results from each of the TCCON sites, indicated by the row title. Each column shows the results from each window, indicated by the title of each column. Each subplot shows the RMSE and χ^2 values for each spectroscopic database indicated in the x-axis, with the blue bars referring to the RMSE values, with magnitudes shown on the left-hand y-axis. The black bars refer to the χ^2 values, with the magnitudes indicated on the right-hand y-axis.

Since all trace gases are fit simultaneously in all of the windows, there no specific metrics associated with $^{13}CH_4$ ~~and .~~ $^{13}CH_4$ ~~from cases where parameters errors have been introduced,~~ in this study is fit in windows 1 and ~~the original unperturbed cases. This linear regression is represented in two types of figure, the first qualitatively shows the correlation between perturbed and unperturbed cases for all windows , spectroscopic databases and TCCON sites. The second figure type shows the linear regression and correlation statistics (slope, intercept, coefficient of determination and standard deviation) for the correlation plots in the first figure. These statistics are shown for all windows, spectroscopic databases and TCCON sites. All these results and~~ 4.

3.2 Quantification of variance between windows and databases

The entire time series available for this study for each TCCON site are shown in Figs. 3, 4, 5 and 6. Qualitative inspection of these figures shows scatter between all windows for each database, further the HITRAN, GESIA and SEOM-IAS databases show significant positive bias w.r.t. the standard deviation of the reference TCCON retrieval, indicated by the dashed black lines. Quantitative metrics for these figures are shown in ~~Appendix C, and a summary, highlighting the impact of retrieval parameter uncertainty is shown in sect 3.5~~Fig 7.

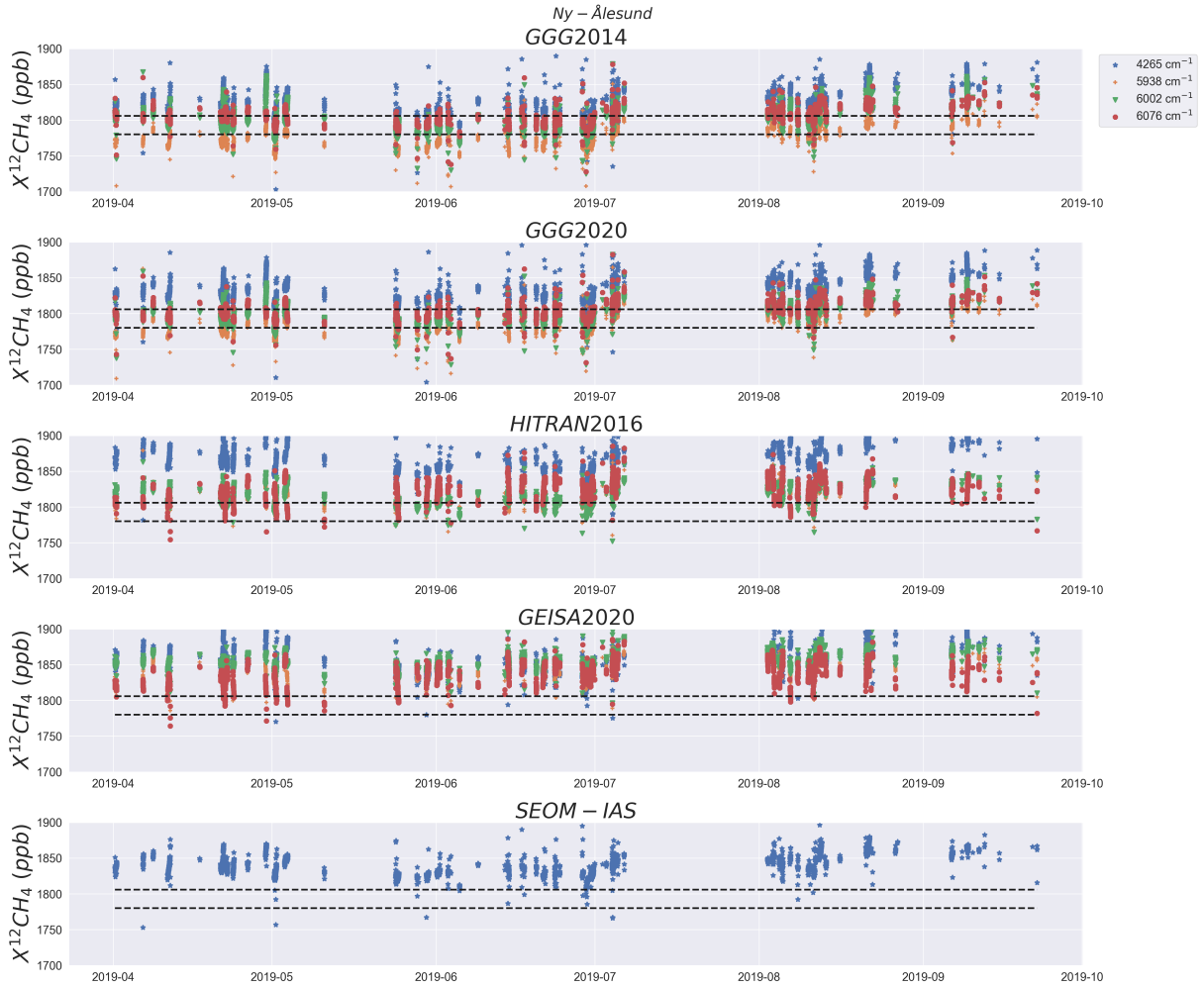

Figure 3. Retrieval time series for $^{12}CH_4$ DMFs from the Ny-Ålesund site. Each panel indicates retrievals from each spectral window (indicated in the legend) from a specific spectroscopic database, indicated in the panel title. Blue stars show retrievals from band 1, yellow pluses are band 2, green triangles are band 3 and red circles are band 4. The standard deviation about the reference TCCON retrievals are indicated by the horizontal dashed lines.

3.1 ~~Averaging kernels~~

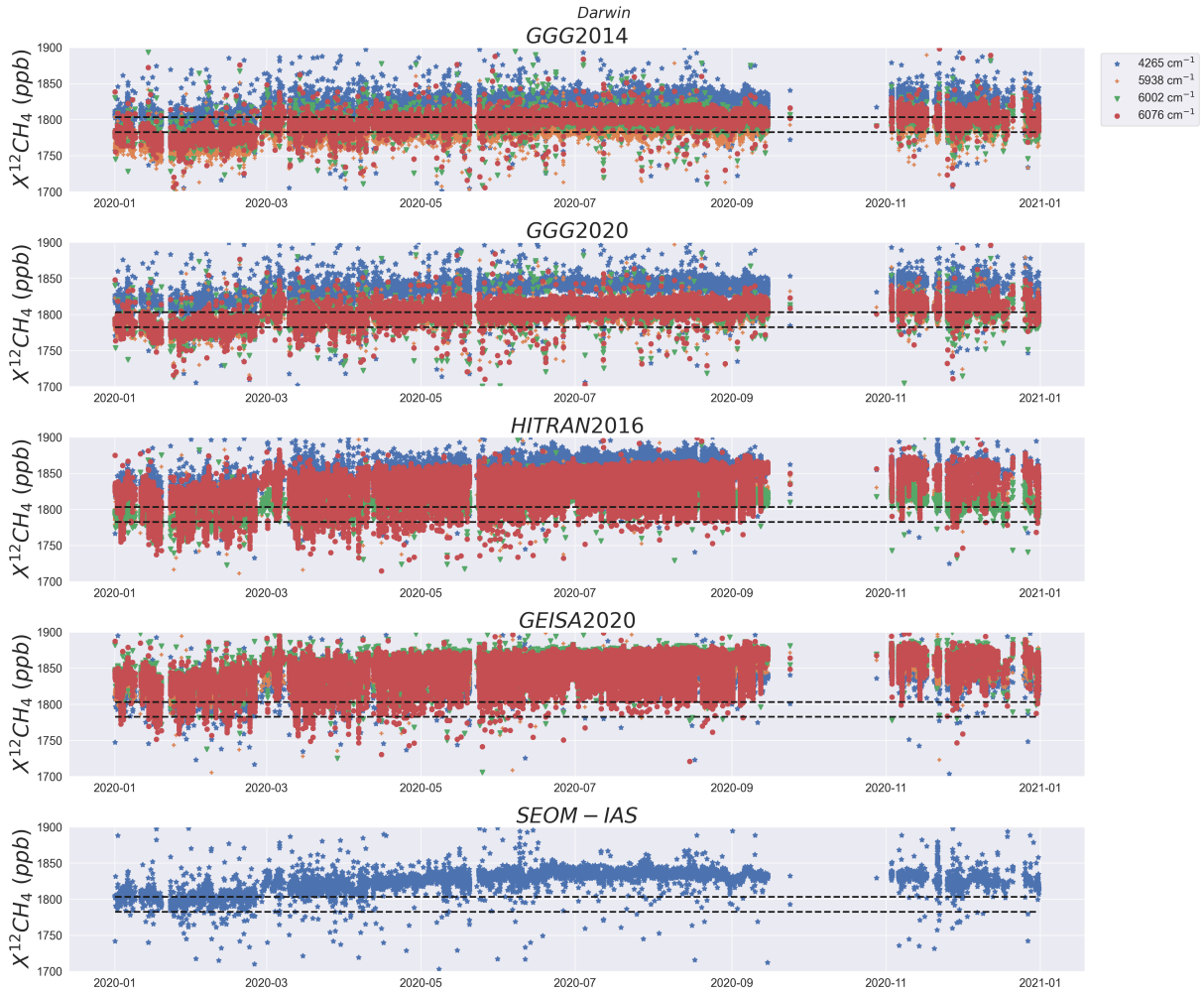

Figure 4. As Fig. 3, but for retrievals from the Darwin TCCON.

~~Figure 1 shows example column averaging kernels for retrievals of $^{12}CH_4$ and $^{13}CH_4$ using windows 1, and 4-6 from selected observations at both Tsukuba and Ascension Island.~~

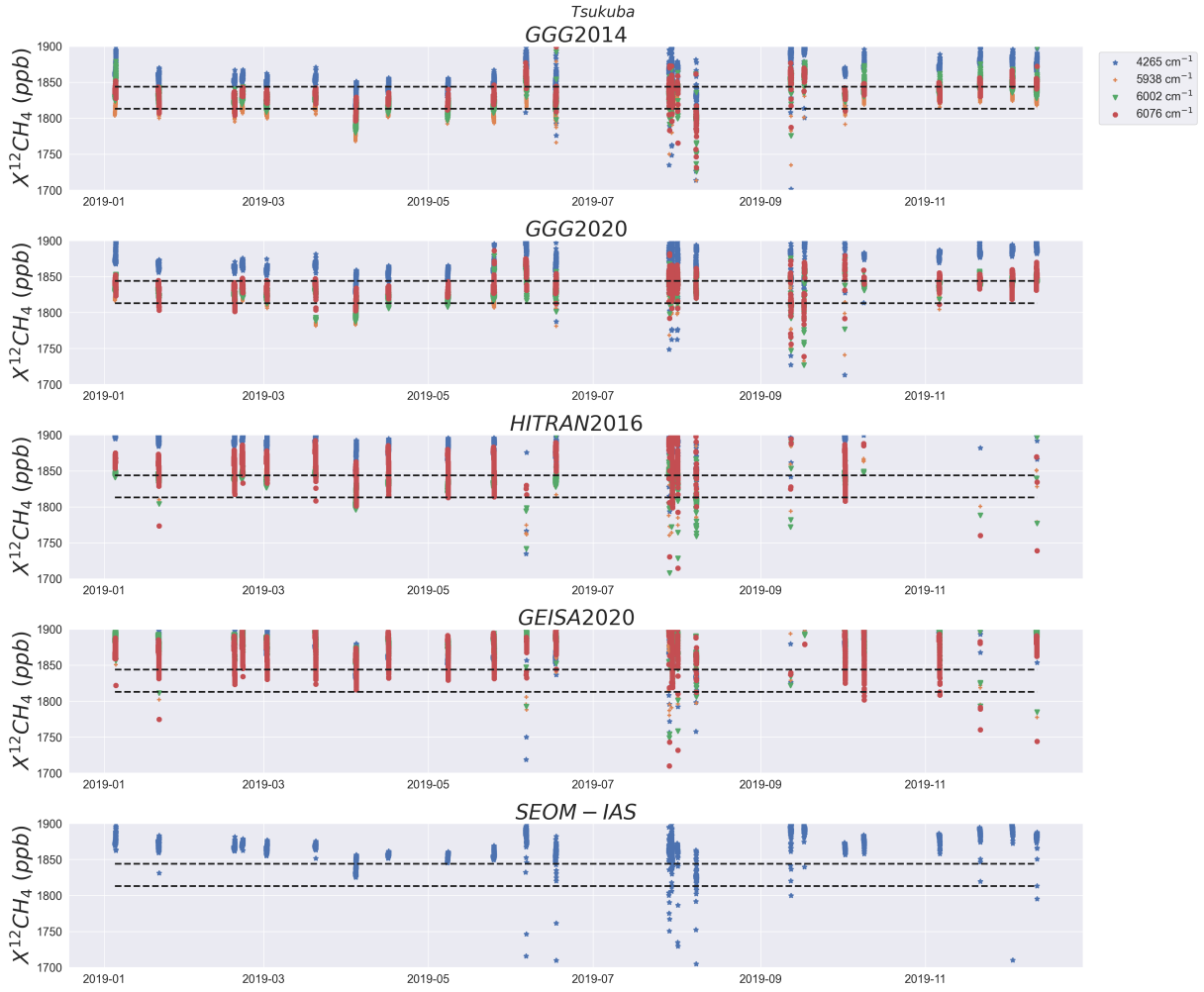

Figure 5. As Fig. 3, but for retrievals from the Tsukuba TCCON.

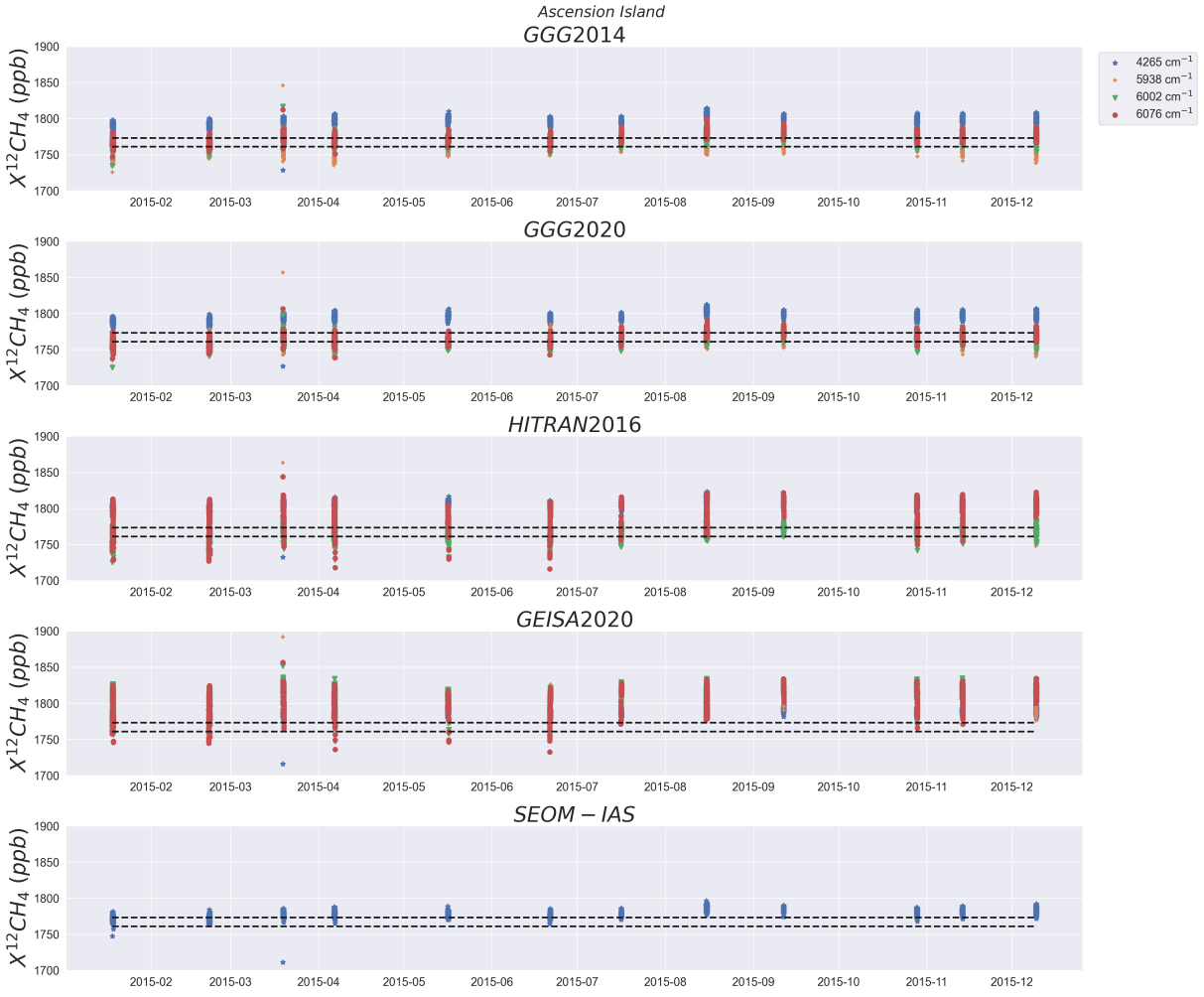

Figure 6. ~~Column averaging kernels~~ As Fig. 3, but for ~~typical~~ retrievals ~~of $^{12}CH_4$ and $^{13}CH_4$~~ from the ~~Tsukuba TCCON site (left) and~~ Ascension Island TCCON~~site (right) using the internal TCCON spectral database.The legend indicates the spectral window, for which the averaging kernels were calculated.~~

The metrics used in Fig 7 indicate the the bias for $^{12}CH_4$ ~~averaging kernels for both windows and both sites show little variation, and are similar to the CH_4 averaging kernels shown in (Wunch et al., 2011).The $^{13}CH_4$ averaging kernels show larger variation in the upper atmosphere, especially in the Ascension Island case, however this is not significant given the low concentration of $^{13}CH_4$ in the upper stratosphere. The shape of $^{13}CH_4$ averaging kernels is very similar to the shape of averaging kernels of CO from TCCON (Wunch et al., 2011), for all cases analysed in the present study. The similarity of the averaging kernels for the different windows shown in Fig~~ retrievals each database and window w.r.t the reference retrieval (Norm Abs Mean), and the presence of any large deviations (RMSE). These metrics are normalised by the retrieval uncertainty of the reference retrievals a weighted average of windows 2, 3 and 4 from GGG2014, thus we assume any biases with values

greater than 1 ~~shows that the total columns retrieved from different fit windows can be compared directly, and that biases between windows can~~ cannot be attributed to ~~other sources~~uncertainty and are therefore real.

3.1 ~~Transmission fit accuracy~~

~~Example transmission spectra calculated from retrievals of $^{12}CH_4$ and $^{13}CH_4$ from the Tsukuba site in April 2016. Row 1 represents the calculated transmission of the target species ($^{12}CH_4$ for first four columns, $^{13}CH_4$ for the last two columns) using the TCCON spectroscopy database. The first four columns represent windows 1-4 respectively, the last two represent the windows of $^{13}CH_4$. The second row shows the residual transmission between the measured and calculated transmission from the SEOM-IAS database in window 1. Row 3 shows the residual transmission when the HITRAN2016 database is used, row 4 is the GEISA database and row 5 is the TCCON database.~~

~~Figure 2 shows the relative strengths of the absorption of the target trace gases in the selected spectral windows. We see that~~ Firstly the results from Ny-Ålesund, which due to the constant nature of the atmospheric conditions can be considered as a baseline. For window 1~~is a complex region with a large number of absorption lines including strong lines that saturate in the centre, and pronounced spectral overlap of lines. Windows 2-4 all show high levels of absorption but less line mixing/overlapping lines. The absorption by $^{13}CH_4$ in windows 5 and 6 are weak; window~~ , both the NRMSE and Norm Abs Mean values for all of the databases indicate values greater than 1~~contains significantly larger number of spectral lines compared to window 4. Both HITRAN2016 and GEISA2015 show significant residual transmission peaks in all of the windows. Quantitatively, the transmission statistics listed in Table 4 indicate that the SEOM-IAS retrieval has the best fit in window 1, with the TCCON database showing similar values. Note that the fit characteristics of~~ , thus suggesting there are still significant variations in the treatment of spectroscopic parameters in window 1. The HITRAN and GEISA databases show bias deviations twice that of GGG2014, however these values do not indicate any one database is more accurate than the other, but either large differences in spectroscopic parameters or differences in sensitivity to local conditions. Windows 2 & 3 do not show any notable biases apart from the GEISA database which generally shows the largest deviations across all of the windows (except window 1~~are several times worse than any of the other windows explored in this study. We must take into account here that window~~). In window 4, both HITRAN and GEISA show notable deviation from the reference retrievals, which is a surprising result given this window is popular in satellite retrievals of methane (Yoshida et al., 2013). We note the NRMSE and Norm Abs Mean values are similar in the majority of cases, indicating that there is an underlying bias between the database retrievals as opposed to large spikes of differences. Considering the bias deviations across the windows, GEISA is the only example to exceed values of 1 ~~is wide, and that better fits could be obtained by splitting the window~~across all windows, with window 3 showing the largest deviation from the reference value. ~~Note that the column densities for all trace gases are fitted simultaneously, therefore changing the target gas for retrieval purposes (e. g. $^{12}CH_4$ or $^{13}CH_4$) does not change the fit residuals, hence this is why only the transmission values for $^{13}CH_4$ are shown, and no residuals.~~

~~For comparison purposes, Table A1 shows the same fit parameters, as shown in Table 4, but for an example of Ascension Island retrieval in October of 2016. The quality of fit is several times worse for the example of Ascension Island spectra, this is explained in Appendix A.~~

~~The key point is the relative fit values between the windows and spectral databases , which are similar to~~ Secondly considering the dataset from Darwin, the magnitude of the NRMSE and Norm Abs Mean values are typically lower than the equivalents in the Ny-Ålesund dataset. The relative differences between the NRMSE and Norm Abs Mean values between the databases are the same as those shown in ~~Table 4. This implies that the differences observed between the windows and databases exist, irrespective of time and location.Suggesting site and season are not major contributors to biases in window and spectroscopic database. The example transmission spectra shown in Fig 2 were captured with a solar zenith angle of 43°, with a similar air mass to other spectra captured on the same day, and~~ the ~~Ascension Island spectra were captured with a solar zenith angle of 22°, with a similar air mass to the Tsukuba spectra.~~

~~This analysis also shows that the GEISA database does not include any $^{13}CH_4$ lines in window 5, meaning that there will be no further analysis on this window w.r.t GEISA.~~

~~Retrieval fit statistics for the case identified in Fig 1. The RMSE for each spectroscopic database is shown in row 1, with the results for windows 1-4 indicated in columns 1-4. The χ^2 values are shown in row 2 for each window. Window~~ Ny-Ålesund dataset, i.e. GGG2014 shows the lowest differences and GEISA shows the largest, apart from in window 1 ~~Window~~ in which case it is HITRAN. Investigating each window in turn, only HITRAN shows a notable deviation from the standard in window 1 with GGG2020 and GEISA not indicating a significant deviation above the standard noise level (only 0.02 and 0.07 above 1 respectively). For windows 2 ~~Window~~ & 3~~Window~~ , only the GEISA database shows a significant bias with

					TCCON: $4.438\text{x}10^{-3}$	TCCON: $3.076\text{x}10^{-3}$
					HITRAN: $6.803\text{x}10^{-3}$	HITRAN: $3.747\text{x}10^{-3}$
					GEISA: $5.678\text{x}10^{-3}$	GEISA: $3.910\text{x}10^{-3}$

respect to the standard, as with Ny-Ålesund site. Again in window 4 ~~RMSE SEOM: $4.268\text{x}10^{-3}$ SEOM: nan~~

TCCON: $3.846\text{x}10^{-3}$	TCCON: $2.680\text{x}10^{-3}$	TCCON: 0.392	TCCON: 0.146	TCCON: 0.0218	TCCON: 0.132	
HITRAN: $5.392\text{x}10^{-3}$	HITRAN: $3.578\text{x}10^{-3}$	HITRAN: 0.922	HITRAN: 0.216	HITRAN: 0.0414	HITRAN: 0.235	
GEISA: $6.01\text{x}10^{-3}$	GEISA: $3.722\text{x}10^{-3}$	GEISA: 0.642	GEISA: 0.235	GEISA: 0.0532	GEISA: 0.254	
~~SEOM: nan~~	~~SEOM: nan~~	~~χ^2~~	~~SEOM: 0.363~~	~~SEOM: nan~~	~~SEOM: nan~~	~~SEOM: nan~~

~~Note that the RMSE and χ^2 values for the $^{13}CH_4$ retrievals are identical to those indicated for $^{12}CH_4$ in the same window, and are therefore not repeated in Table 4.~~

3.1 ~~Retrieval accuracy~~

~~Figure 3 shows a time series of 40 DMFs of $^{12}CH_4$ from measurements made on the 1st of April 2016 at the Tsukuba TCCON site. The top panel shows the time series over the course of the day for each spectral window and databasein consideration. We see here that the maximum bias in retrieved $^{12}CH_4$ DMFs is roughly 50 ppb, between the~~ only the HITRAN and GEISA ~~6002 cm^{-1} windows. The statistics in Table 5 suggest that window 3 has the largest deviation in DMFs~~ databases show notable deviation from the standard, again suggesting the spectroscopic parameters in window 4 still have significant uncertainty w.r.t ~~. spectroscopic databases, while window 1 has the lowest deviation. In general Table 5 suggests that there are significant variations in the retrieved DMFs in both spectral windows and spectral databases. The middle panel in Fig. 3 reveals a clear and constant bias between the reference values and the other windows, of up to~~ windows 2 ~~%.~~ & 3. The implication of the Darwin

results w.r.t those from Ny-Ålesund are that either or both the differences in the instrument setup and the local conditions impact inter-window/spectroscopic database biases.

~~Table 5 suggests that~~ The results for the Tsukuba retrievals are very similar to those shown for Ny-Ålesund, with GGG2014 not showing any significant differences except in window 1~~shows the least variation, and window 3 has the most (largely driven by the GEISA retrievals). However, the inter-window variation suggests the least variation from the GEISA retrievals; the HITRAN retrievals show the most.The bias values from the equivalent TCCON windows in general show the largest biases from the GEISA retrievals. However window~~ , as with the other sites HITRAN shows deviation in windows 1 ~~from the SEOM-IAS database shows the largest bias in this regard.~~ and 4, and GEISA showing the largest differences apart from in window 1. However, the main difference is with the GGG2020 database, as with the other TCCON sites the normalised absolute mean shows deviation in windows 1 and 4, however the NRMSE indicates significant differences in all windows, suggesting there are a small number of retrieval cases that have large biases w.r.t the standard values. This behaviour is not replicated in the other TCCON sites.

~~Retrieval uncertainties shown in the bottom panel of~~ Finally, all results from the Ascension Island measurements indicate no deviations of any significance, contrasting with the results from all other sides. We note the standard deviation about the reference TCCON retrievals in Fig~~3 suggest a typical range of between 5 and 10 ppb, with the GEISA and HITRAN retrievals showing the highest errors. These errors are significantly lower than the persistent differences noted between the windows, meaning that these biases cannot be attributed to random retrieval uncertainties, and are likely due to differences~~ 6 is smaller than any of the other TCCON sites. This suggests constant retrievals in methane over the course of the year at Ascension Island, and therefore limited opportunity for biases to form.

The results in Fig 7 clearly indicate that in the ~~spectroscopic~~ cases where deviations exist, they are reflected in all of the TCCON sites (when significant), implying that despite the fit differences shown in Fig 2 these biases cannot (purely) be attributed to errors in the TCCON instruments, but given the consistency of the deviations we can attribute these differences to spectroscopic parameters. Figure 7 indicates that there are significant differences between SEOM-IAS, GEISA and HITRAN databases w.r.t. the GGG databases, which show less deviation. This is not surprising since the reference values are based on GGG2014, and GGG2020 is built upon GGG2014, however this is not the case in window 1 where larger deviations are observed. This suggests that knowledge of spectroscopic parameters in window 1 is still not as settled as the other windows which have been routinely used in TCCON. It is difficult to assess all of the differences between the databases, due to the range of parameters used; there are some papers which describe the sources of the spectral lines for each of the databases (Brown et al., 2013; Jacquinet-Husson et al., 2016), but specifics are limited due to the size of the databases. Complexity is added by the fact that several of these databases state that data is drawn from the same sources (Albert et al., 2009; Nikitin et al., 2015, 2017 , however these papers go on to say that not all of the lines from these studies are implemented based on in house assessments of fit quality. The implication being that it is challenging to specifically identify where spectroscopic parameter differences occur between the databases.

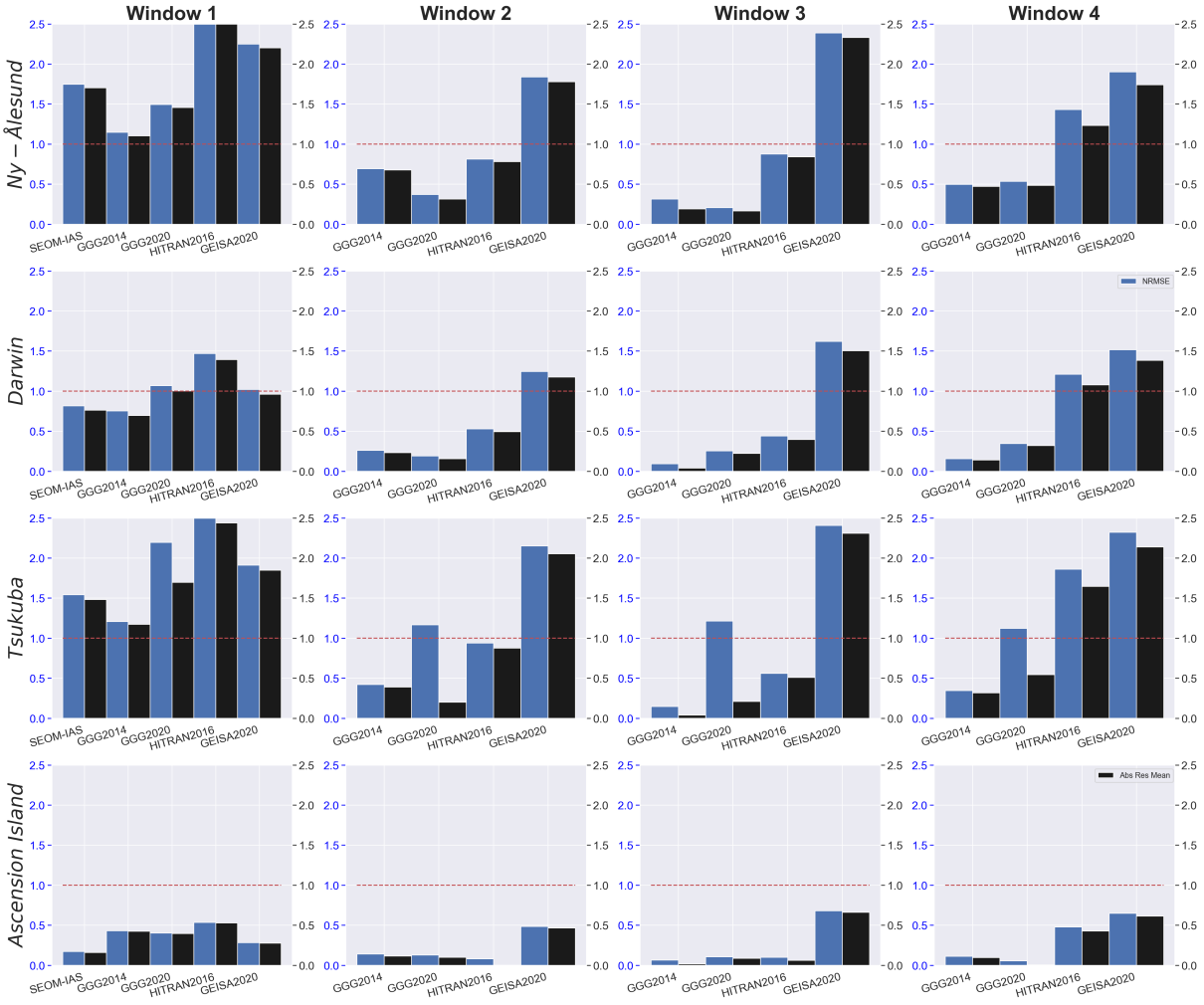

Figure 7. ~~Retrieval time series~~ Bar plot indicating NRMSE and Normalised Absolute mean residual difference values for $^{12}CH_4$ ~~DMFs~~ retrievals from ~~the Tsukuba~~ each TCCON site~~on 01/04/2016. The top panel indicates the retrieved DMFs of $^{12}CH_4$ in ppb for differing spectral windows~~, each window and each spectroscopic ~~databases. The spectral windows are differentiated by line style, as shown~~ database under consideration in this study with respect to the ~~legend in the top right corner~~original TCCON methane retrieval window. ~~The databases are differentiated~~ Each row shows data from each TCCON site, as indicated by ~~colour~~the y-axis titles, and each column shows results from each window, as indicated ~~in~~ by the ~~right of the middle panel~~column title. ~~The middle panel~~ Each subplot shows the ~~relative difference of~~ NRMSE (the ~~retrievals with respect to retrievals from window 4 of~~ blue bars, magnitude shown by the ~~TCCON database in ppb~~left-hand y-axis) and Abs Res Mean (the black bars, ~~illustrating~~ indicated by the ~~persistent behaviour of~~ right-hand y-axis) values for each spectroscopic database as indicated by the ~~spectroscopic-dependent and fit-window dependent differences~~x-axis. The ~~bottom panel shows~~ horizontal red-dashed lines indicated the ~~total retrieval uncertainties in ppb~~magnitude of 1, the value where we assume the bias values to be significant.

~~Statistics on 40 retrievals from the Tsukuba site on 01/04/2016 based on metrics identified in retrieval abundances subsection~~
505 ~~of section 2.2. The first row indicates the standard deviation of the retrieved DMFs from each window under study in this paper,~~

with the target indicated for each window. The second data row indicates the standard deviation of the retrieved abundances of $^{12}CH_4$ for all windows present in each spectroscopic database, the third data row is as the second row, but for $^{13}CH_4$. The fourth to ninth data rows indicate the retrieved mean of the DMF for each window against the retrieved mean of the equivalent window using the TCCON spectroscopic database, with the window in question highlighted in the rows, and the spectroscopic database indicated in the columns. Window 1 ($^{12}CH_4$) 2 ($^{12}CH_4$) 3 ($^{12}CH_4$) 4 ($^{12}CH_4$) 5 (For $^{13}CH_4$) 6 (DMFs there is no obvious reference value available, since $^{13}CH_4$) σ_{window} (ppb) 8.98 17.5 22.5 12.6 0.589 1.64 TCCONHITRAN GEISA is not typically retrieved from TCCON. We therefore chose to use GGG2014 window 1 as a reference in order to investigate window deviations. We found that apart from SEOM-IAS 16.5 20.0 9.15 N/A 1.09 0.389 N/A N/A Database bias (ppb; window 1) bias (ppb; window 2) bias (ppb; window 3) bias (ppb; window 4) bias (ppb; window 5) bias (ppb; window 6) which showed deviation below the noise level from every TCCON site, every other case showed notable levels of deviation ranging from 1.5-5. Here we cannot attribute these disagreements purely to spectroscopic differences since $^{13}CH_4$ retrievals will be subject to high noise levels.

Considering a different set of retrievals, in this case 79 from the Ascension Island siteon 01/10/2016, the statistics of which are highlighted in Table 6. These are shown to be similar in magnitude to those indicated in Table 5 (exemplified by the σ_{window} values), but are also shown to vary i. e in some cases magnitude increases, while others decrease. The $\sigma_{inter-window}$ values show similar magnitudes in both Tables 5 and 6, with HITRAN showing the largest inter-window variation, and GEISA the lowest. In general the bias values are similar in Table 5 and Table 6, however there are some differences

3.1 Impact of local condition changes on variance between windows and databases

The TCCON sites used in this study were picked to have a wide range of conditions, with Ny-Ålesund capturing spectra in largely unvarying conditions with high SZA and low water vapour, while Ascension Island is similar in unvarying conditions although with higher background water vapour conditions and lower SZAs. This is contrasted by Darwin and Tsukuba which capture spectra under a wide range of SZAs and highly variable water vapour conditions (see Table 3). It has been shown (Wunch et al., 2011) that the variability of local conditions can have an impact on the accuracy of TCCON retrievals (through the apriori data). We therefore investigate in this section if varying local conditions (specifically, water vapour, SZA and temperature) affect each window in each spectroscopic database differently.

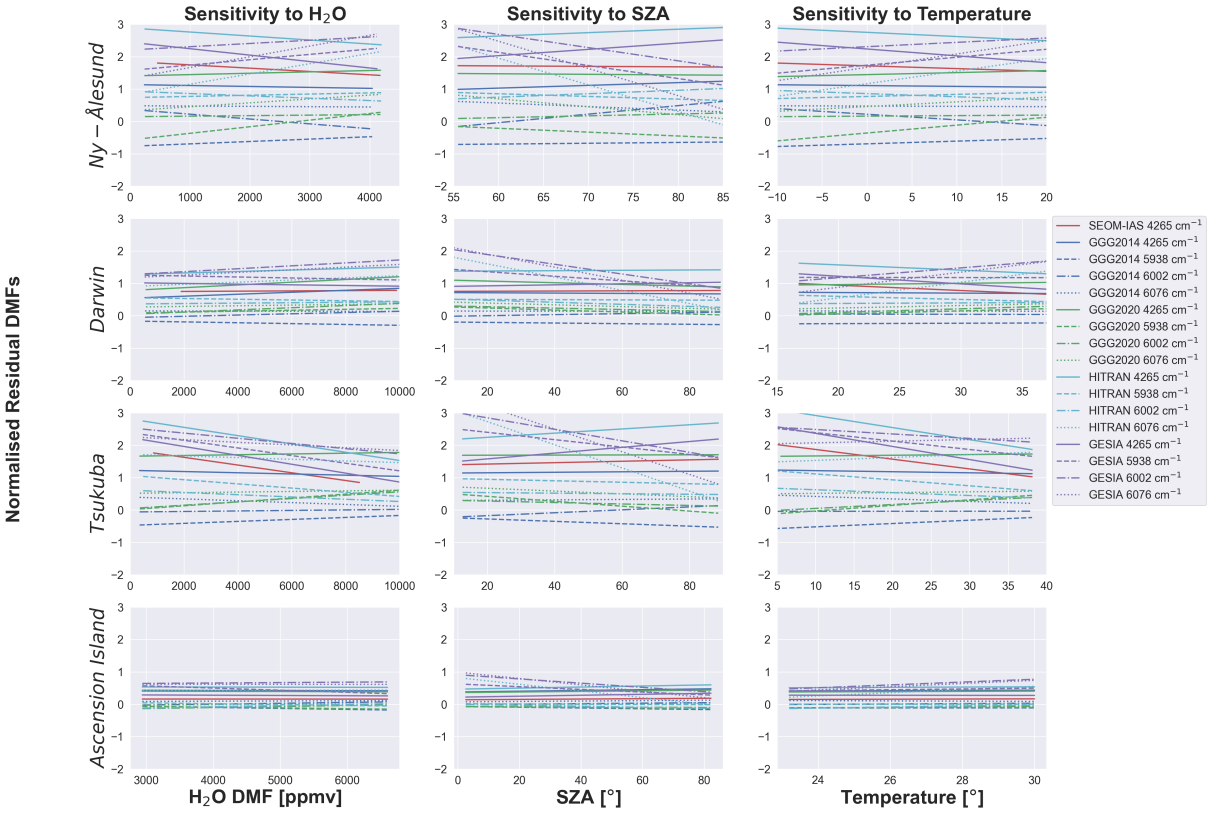

Figure 8. The sensitivity of water vapour, SZA and temperature variations on retrieved $^{12}CH_4$ DMFs from each TCCON site, spectroscopic database and windows. Each subplot shows the linear fit of the normalised residual between the retrieved window/spectroscopic database DMFs and the TCCON reference DMFs, with the fit window and spectroscopic database indicated by the legend. Each row of the figure shows data from each TCCON site as indicated in the y-axis, and each column shows the sensitivity to a specific condition as shown in the title.

The qualitative distributions indicated in Fig. 8 are explored quantitatively in more detail in Figs 9, 10, and 11. First considering the impact of SZA variations in window 1 across all sites, there is no clear pattern in the correlations. For example~~.~~ ~~there is a significantly larger bias for~~ , GGG2014 at Ny-Ålesund and Ascension Island shows a weak correlation of ~0.25, yet no correlation at either Darwin and Tsukuba. This pattern is repeated for all databases except GEISA2020, which shows a weak correlation across all TCCON sites. For window 2 ~~in HITRAN,~~ we see weak to strong correlation in all databases across all sites, except for a few cases (e.g. HITRAN at Darwin and Ascension Island). Window 3 shows high levels of correlation to SZA variations w.r.t. all sites, with Ny-Ålesund and Ascension Island showing particularly notable correlations, especially in the GGG2014 and ~~lower for window 4 in HITRAN~~GEISA2020 databases. Window 4 ~~bias for GEISA is also significantly lower. These results indicate that we can expect variations in retrieved methane biases depending on TCCON site and time of year.~~ shows large correlations for all databases in the Ny-Ålesund retrievals especially, but large negative correlations across all sites

with the HITRAN and GEISA databases. Overall the results in Fig 9 indicate the retrieval biases w.r.t the reference TCCON retrievals are sensitive to SZA variations. The Ny-Ålesund site shows the largest sensitivity of all of the sites considered in this study. This could be explained by the fact that Ny-Ålesund operates at higher SZA angles than any of the other TCCON sites, meaning the retrieval path length will be longer, potentially allowing for more errors to creep into the retrievals. However, the results from Ascension Island, which operates at lower SZAs than any of the other TCCON sites considered in this study also indicates large correlations, suggesting further complexity.

Statistics on 79 retrievals from the Ascension Island site on 01/10/2016 based on metrics identified in retrieval abundances subsection of section 2.2. The first row indicates the standard deviation of the retrieved DMFs from each window under study in this paper, with the target indicated for each window. The second data row indicates the standard deviation of the retrieved abundances of $^{12}CH_4$ for all windows present in each spectroscopic database, the third data row is as the second row, but for $^{13}CH_4$. The fourth to ninth data rows indicate the retrieved mean of the DMF for each window against the retrieved mean of the equivalent window using the TCCON spectroscopic database, with the window in question highlighted in the rows, and the spectroscopic database indicated in the columns. Window The sensitivity of each window to water vapour variation is explored in Fig 10. For window 1($^{12}CH_4$) 2 ($^{12}CH_4$) 3 ($^{12}CH_4$) 4 ($^{12}CH_4$) 5 ($^{13}CH_4$) 6 ($^{13}CH_4$) σ_{window} (ppb) 10.6 16.6 21.2 14.8 0.981 2.79 TCCON HITRAN GEISA , there is weak sensitivity to water vapour variations at the Ny-Ålesund and the Darwin sites, with opposite databases showing greater sensitivity. The Tsukuba site shows large negative correlations for the HITRAN, GEISA and SEOM-IAS 16.3 19.4 11.1 N/A 1.83 2.30 N/A N/A Database bias (ppb; window 1) bias (ppb; window databases, while Ascension Island shows very little correlation across all databases. Window 2) bias (ppb; window 3) bias (ppb; window shows large correlation magnitudes, with the Ny-Ålesund and Tsukuba both showing correlations >0.5 in several cases. In general, all databases in window 2 shows correlation values >0.25 except for a small number of cases, most notably at the Darwin site. Different patterns are observed with windows 3, where Ny-Ålesund shows some significant negative correlations, while Ascension Island indicates sensitivity across all databases (except GEISA). Darwin and Tsukuba show opposite behaviours with large positive correlations at GGG2014 and GGG2020 at Darwin, but large negative biases with the HITRAN and GEISA databases at Tsukuba. For window 4) bias (ppb; window 5) bias (ppb; window 6) , notable correlations are observed for GGG2020, HITRAN and GEISA at Ny-Ålesund, but in general there are no other correlations of note across the other TCCON sites (except for GGG2014 at Tsukuba). These results are curious, we know Darwin, Tsukuba and Ascension Island have much higher background water vapour levels and variability ∼x3 than Ny-Ålesund. Yet, Ny-Ålesund shows larger correlation in some cases than any of the other sites with high water vapour concentrations. Tsukuba has a background water vapour content less than that of Darwin, but exhibits variability ∼x2 that of Darwin, and for Tsukuba there is much greater indication of bias sensitivity to water vapour. Thus suggesting that the variability of water vapour in the atmosphere is more significant for retrieval biases, as opposed to high background levels.

For further analysis on the biases presented in Fig 3 and Tables 5 and 6, we also show additional retrieval statistics for 40 retrievalsfrom Tsukuba on 07/07/2016 (Table B1), and 243 retrievals from Ascension Island on 23/08/2016 (Table B2). Comparing the statistics from Fig. 3 and Tables 5, 6, B1 and B2, we note similar magnitudesin all of the presented statistics, and similar magnitudes in the differences when comparing the results from different windows or spectroscopic database. For

example the σ_{window} value in window 1 is between 8.98 and 10.6 ppb depending on TCCON site and time of year of retrievals, but for The results for retrieval bias sensitivity to variations in temperature are shown in Fig 11. Comparisons of Figs 10 and 11 show similar results in both cases, for example, window 3 it is between 21.2 and 23.7 ppb. In the cases shown in this study, σ_{window} is at a minimum in window 1 , and at a maximum in at the Ny-Ålesund site shows almost identical results. This suggests for the Ny-Ålesund site, water vapour and temperature variability occur on similar time scales, this result is expected as the atmosphere can hold more water with rising temperatures. Similar patterns are apparent at the Tsukuba site with some notable exceptions, although these exceptions occur in cases with low bias sensitivity (e.g. GGG2014 window 3,), meaning these are unimportant. However, this similarity is not as apparent at the Darwin site, with window 3 showing up to roughly x2.5 larger deviation than window 1. Windows 2 and 4 show more variation, and often show similar magnitudes. The implications of these results are that windows 1 and 3 are more consistent across the databases, and windows 2 and 4 are less so. $\sigma_{inter-window}$ results consistently show the GEISA2015 database has the lowest deviation in $^{12}CH_4$ DMFs across all bands, but also show the most variation across sites and season (4.25 ppb) . HITRAN2016 shows the highest $\sigma_{inter-window}$ results, and higher retrieval bias sensitivity to water vapour than to temperature variation. Indeed, Darwin does not indicate any cases with retrieval bias correlation >0.25, (unlike any of the other sites). The key exception to this pattern are the TCCON database is in between, but shows almost no variation in values across sites and seasons. Considering the biases of each spectral window from each spectroscopic database against the equivalent window from the TCCON spectroscopic database , there is evidence of some patterns emergingresults from Ascension Island, where the values for water vapour and temperature sensitivity are significantly different. We note in this case that the temperature variation at Ascension Island (Table 3) is very small, which could explain these differences.

In general, there is no clear case of one window, database or TCCON site showing clear sensitivity over and above than any of the others in all cases, meaning one site or database is not especially sensitive than the others. However there are clear indications of sensitivity to variations in the local conditions which vary between window, database and TCCON site, in some cases very strong correlations. In general, the pattern is that variability in the local conditions causes window and database biases, rather than extreme conditions by themselves. For example, the HITRAN2016 database shows the lowest bias in each window w. r.t. the TCCON database, while the GEISA2015 database shows the highest and Ascension Island has the least varying conditions of all of the sites, and also shows the most constant sensitivity to varying conditions. While Tsukuba has some of the most variable conditions and also indicates some of the most variability when assessing water vapour variability. This assessment is not perfect, since Ny-Ålesund also shows significant dependence on local conditions, while having less variability than Darwin or Tsukuba. However, Ny-Ålesund spectra are captured at high SZA meaning lower SNR and more susceptibility to interfering elements.

We also note when calculating the Pearson's correlation coefficent for GGG2020 values for window 1 for all spectroscopic databases consistently shows largely constant values across all TCCON sites and seasons. However, there is also significantevidence of changing behaviours, window 4 especially varies by as much as 300% between sites and seasons. The results from this analysis suggest that window 1 is the most consistent and is less sensitive to changing conditions, while other windows show

610 ~~much more variation with differing conditions.~~ at the Tsukuba site, large 'p' values were found, indicating these results are not statistically significant.

~~For~~

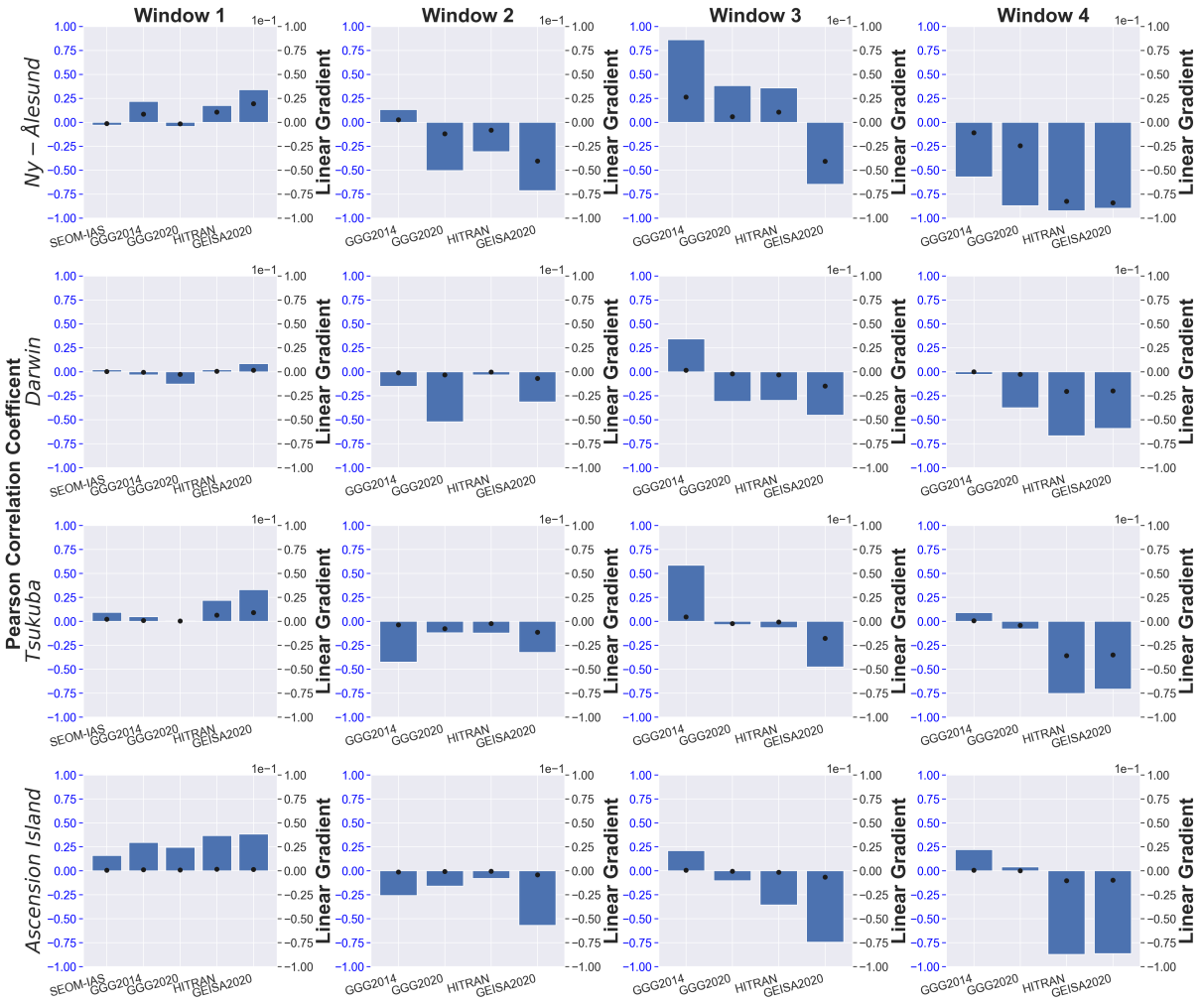

Figure 9. Bar chart indicating the statistics behind the sensitivities to SZA variations shown in Fig 8. Each row indicates the results from a TCCON site, as indicated by the y-axis label, each column shows the results from a particular window as shown by the column title. The blue bar plot show the Pearson correlation coefficent, with the left-hand blue y-axis values the appropriate scale. The black dots showing the linear gradient of the linear fits from Fig 8, with the right-hand black y-axis values as the scale.

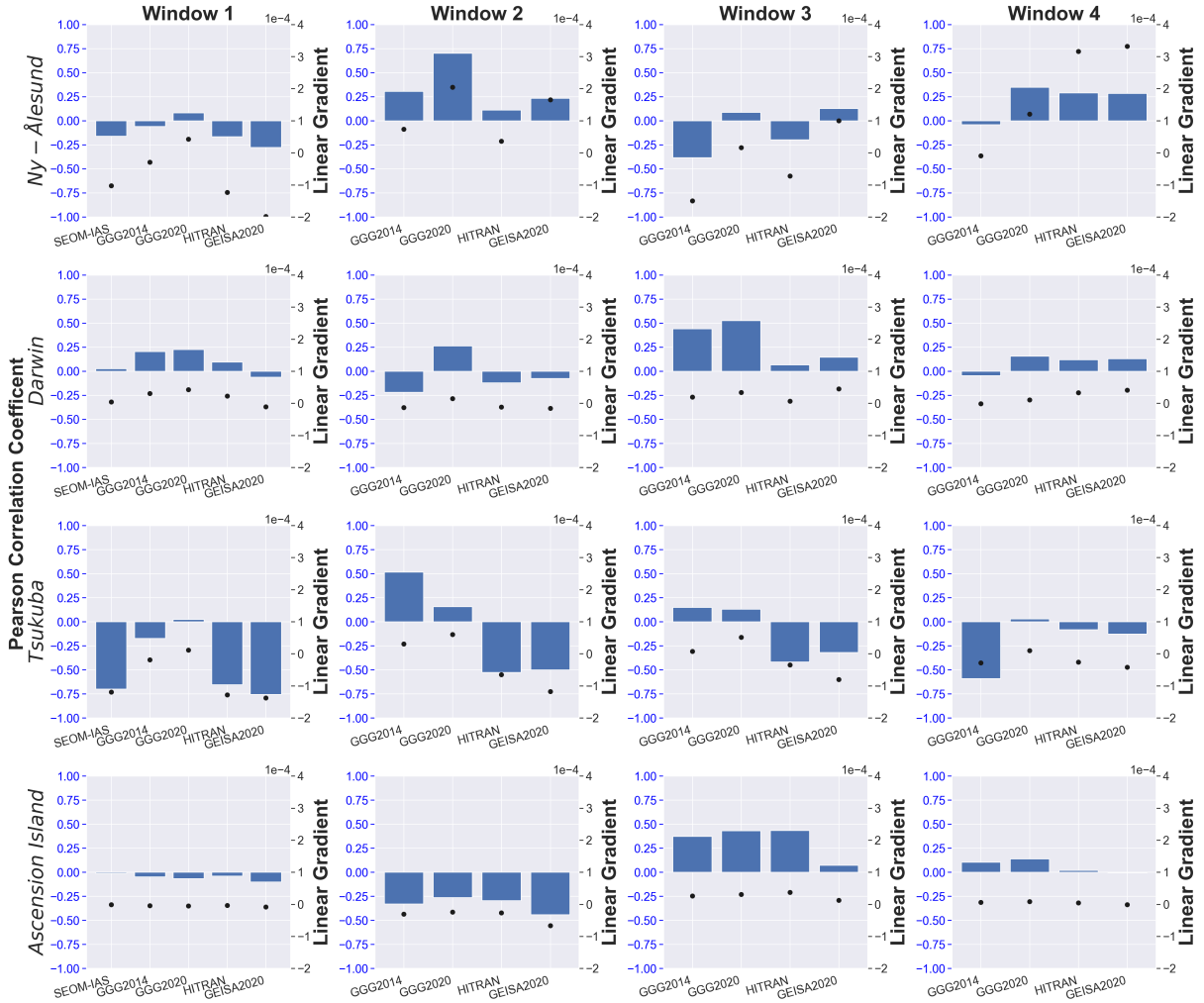

Figure 10. As Fig 9, but showing the sensitivities to water vapour variations.

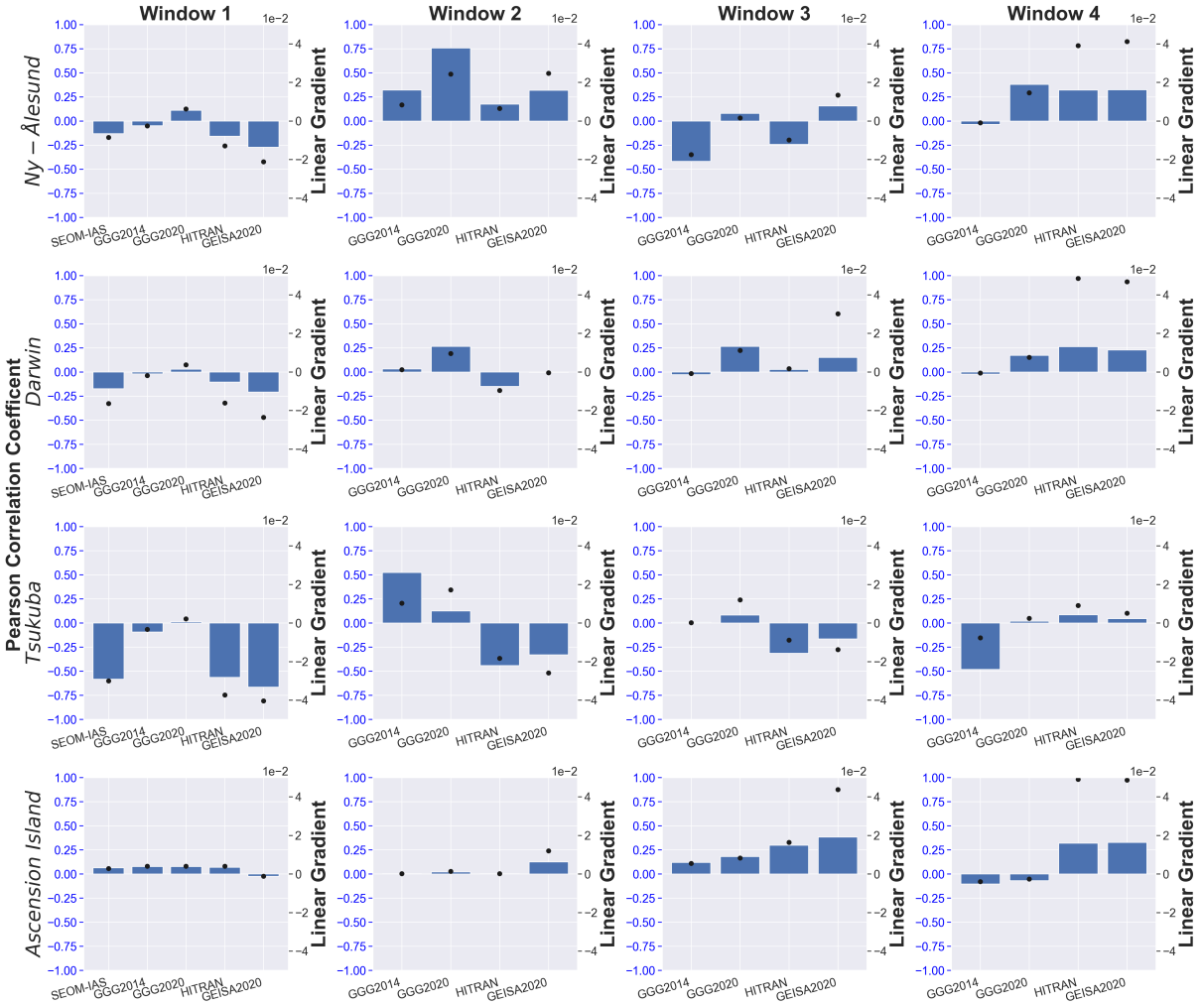

Figure 11. As Fig 9, but showing the sensitivities to temperature variations.

A similar analysis for retrieval bias sensitivities for $^{13}CH_4$ ~~DMFs we see similar results to~~ indicated high levels of sensitivity to SZA variation, especially those retrievals from Ny-Ålesund where SZAs are high. There are some windows that indicate no correlation, but the majority had values greater than 0.3. W.r.t water vapour and temperature variation, these results are mixed with different windows and databases at different sites indicating different results. However there is a general trend of sensitivity to water vapour and temperature variations, with only a small number of cases indicating no correlation. These results suggest $^{13}CH_4$ retrievals are more sensitive to changing conditions than $^{12}CH_4$~~DMFs, window 5 typically shows the least variation, and the GEISA2015 database shows the largest differences~~, which is the expected result.

3.2 Calculation of δ^{13}C values

~~Based on Eq 2, we can calculate~~ The calculation of the $\delta^{13}C$ values ~~for both Tsukuba and Ascension Island TCCON sites for the days shown in this study, this allows to quickly determine how accurate any retrievals~~ (Eq 2), can give some insight into the accuracy of $^{13}CH_4$ ~~DMFs from TCCONare. Here we used the same spectral windows to calculate these values, i. e. windows 1 and 5, and windows 4 and 6. For the~~ retrievals from TCCON, as well as the impact of local condition variations on these retrievals. $\delta^{13}C$ ~~values we calculate an averaged value for the whole day.~~

~~Daily averaged values of $\delta^{13}C$ from both TCCON sites for two $^{12}CH_4$ and $^{13}CH_4$ window combinations for each spectral database.~~

	TCCON	TCCON	HITRAN	HITRAN	GEISA	SEOM
~~$\delta^{13}C$~~	~~windows 1 & 5~~	~~windows 4 & 6~~	~~windows 1 & 5~~	~~windows 4 & 6~~	~~windows 4 & 6~~	~~windows 1 & 5~~
~~Tsukuba 01/04/2016~~	~~-116‰~~	~~-1.52‰~~	~~-59.1‰~~	~~-33.1‰~~	~~-193‰~~	~~-109‰~~
~~Tsukuba 07/07/2016~~	~~-173‰~~	~~74.5‰~~	~~-159‰~~	~~296‰~~	~~-202‰~~	~~-143‰~~
~~Ascension Island 23/08/2016~~	~~-108‰~~	~~-92.4‰~~	~~-104‰~~	~~-8.47‰~~	~~-297‰~~	~~-95.0‰~~
~~Ascension Island 01/10/2016~~	~~-115‰~~	~~43.6‰~~	~~-46.7‰~~	~~160‰~~	~~-134‰~~	~~-84.2‰~~

~~Table 7 shows that the $\delta^{13}C$ values calculated from the windows 1 and 5 combination are partially consistent across sites and dates (with the exception of the July retrievals from Tsukuba), while the values calculated from windows 4 and 6 show much more variation. However, there is still significant variation across all cases that cannot be accounted for purely by precision errors. We therefore assert that in the case of TCCON retrievals, the dominant error in $\delta^{13}C$ retrievals are spectroscopic errors. It is also clear that there is still not possible to make useful retrievals~~ is calculated for all TCCON sites using all combinations of windows from all databases in Table 5, using averaged $^{12}CH_4$ and $^{13}CH_4$ for the whole time series available for each TCCON site. There are two factors to look for in the calculation of $\delta^{13}C$ ~~at this time, with both improvements in spectroscopic parameters and retrieval accuracy necessary.~~

3.3 ~~Sensitivity analysis~~

3.2.1 ~~Local condition variations~~

~~Here we investigate if locally changing conditions impact biases between spectroscopic~~ , firstly the bias w.r.t. the accepted atmospheric average of -47‰ and the consistency of the calculated values across databases and windows~~, as described in sect 2.4.1. Firstly sensitivity to variations in water vapour concentrations are considered in Table 8 below.~~ .

Table 5. ~~Linear relationship expressed at the coefficient~~ Averaged values of ~~determination (R^2) between daily variations of water vapour for each~~ $\delta^{13}C$ from all TCCON ~~site and day considered in this study, and the bias of~~ sites for all possible $^{12}CH_4$ ~~DMFs against the 'reference value'~~ and $^{13}CH_4$ window combinations for each spectral database.

~~The coefficients of determination shown in Table8 generally indicate that there is limited or no relationship between the variability of wa~~									

~~The results shown in Table 9 closely align with those shown in Table 8, in that the Ascension Island October 2016 case shows~~
645 ~~a number of cases with strong linear correlation, while the majority of the Tsukuba retrievals largely indicate no relationship (except in window 4). As with Table 8, the results from window 1 show the weakest relationships, but the results from window 4 from all spectroscopic databases show strong indication of bias sensitivity to SZA. Therefore these results suggest that biases~~

between spectroscopic databases and windows can vary with changing SZA in specific windows. It is likely not a coincidence that the strongest linear correlations in Tables 8 and 9 occur in the same cases. TableD1 indicates the range of SZAs where spectra were captured for each TCCON site, it clearly shows Ascension Island spectra are captured under a wider range of SZAs than Tsukuba, in addition the October retrievals from Ascension Island have a mean SZA of 50°, and the retrievals from Tsukuba and Ascension Island from other seasons have mean SZA of <50°. The implication is that variations in water vapour have more effect on biases between windows and spectroscopic databases when higher SZAs are involved.

3.2.1 A priori and parameter errors

The analysis for the a priori and parameter errors discussed in sect 2.4.2 is shown in Appendix C, split into results for each of the cases described in Table 3. A summery of these results is presented here.

The effect of adding a 2% profile shift to 5 indicates a wide range of results, which is unsurprising given that we calculate the mean uncertainty on a $^{13}CH_4$ retrieval over all datasets at between 18-25%. However, given that the values indicated in Table 5 are averages, this uncertainty should reduce significantly (by $\sim$ x200 in the case of Darwin), meaning that the precision should be comparable to that of an individual $^{12}CH_4$ retrieval. Firstly considering the retrievals that use $^{13}CH_4$ from window 1, these combinations yield surprisingly consistent results site to site and window to window, except for the a priori methane profiles is shown in Appendix C1. Comparing the results from Table 5 and Table C1, only minor differences are shown, implying that for the case of April 2016 in Tsukuba, adding a 2% bias to the methane profile has minimal impact. Figures C1 and C2 build on this by showing close linear relationships between the unperturbed perturbed retrieved DMFs for all windows, spectroscopic databases and TCCON sites considered in this study, suggesting that biases in the a priori methane profile have minimal effect on window and spectroscopic database biases. When methane profile shapes were switched (Appendix C2), we can see through a comparison of Tables 5 and C2 that there is an impact. For example there is a 9.7% difference in the σ_{window} of HITRAN results which show significant bias at the Ny-Ålesund site, although this is contrasted by the HITRAN results at Darwin and Tsukuba which indicates values very close to what might be expected. Indeed, the results from HITRAN at Ny-Ålesund show results significantly different from those at any of the other sites, which can be explained by $^{13}CH_4$ retrievals showing significantly larger biases (at least x2 any other database), and a very high Pearson's correlation (0.7). The results from GEISA are the most consistent across the window 2, and combinations for all sites, showing a maximum of $\sim$13‰ variation across all window combination which is a 7.2% difference in the TCCON $\sigma_{inter-window}$ remarkable result. For comparison purposes, HITRAN shows $\sim$25‰ variation, GGG2020 $\sim$18‰ variation and GGG2014 $\sim$25-60‰ variation. The variations between databases in the same window combinations are larger than those in-between windows, suggesting variable dependence on local conditions, and thus differences in spectroscopic parameters. Except for HITRAN, all of the databases and windows seem to underestimate the accepted $\delta^{13}C$ values.

The results for ^{12}the $^{13}CH_4$. Figures C3 and C4 elaborate on this impact, showing variationin the responses for each window and database, as well as a lower impact in results from Ascension Island. Appendix C3 shows how uncertainty in the a priori knowledge of water vapour affects retrieval biases; comparisons between Tables 5 and C3 show minimal differences, with only windows 2 and window 4 showing notable change. However, Table D1 does show the April 2016 Tsukuba case as having

low water vapour concentration and minor variation. Figures C5 combination are highly varied, more so than those shown for the window 1 combinations. For Ny-Ålesund both the GGG2014 and C6 indicate the higher water vapour concentrations and variability in the other cases have more impact, especially in Tsukuba in July. Indicating that uncertainty in the water vapour column affects inter-window/spectroscopic database biases more significantly in high humidity atmospheres. Figures C5 and C6 also show that windows 2 and 4 are the most affected by uncertainty in the a priori water vapour column. The effects of pressure profile uncertainty are shown in Appendix C4; Table C4 indicates significant changes due to this perturbation, with σ_{window} for window 2020 results show high levels of bias and significant variation, while the HITRAN and GEISA results show much lower bias levels and generally consistent results, with the HITRAN window 1 4 showing a 2.4% difference and a 7.5% difference when considering $\sigma_{inter-window}$ for HITRAN. Bias values range combination showing a realistic result. This is contrasted by the results from Darwin, where large biases are observed from all of the databases, but similar levels of consistency between the window combinations. Tsukuba again shows large bias levels between databases and windows, with window 3 showing the most change (1.5% in the case of HITRAN). Building on these results , the linear correlation plots of Figs C7 and C8 show that each site and season have different sensitivities to perturbations in the pressure profile, with window 2 generally indicating the most sensitivity . Finally, the effects of a 2 K temperature perturbation are investigated in Appendix C5, where again differing bands and spectroscopic databases show different sensitivities. For example, the difference between Table 5 and C5 in the σ_{window} GEISA showing high levels of consistency but large bias. Ascension Island shows similar results to Darwin (except for the HITRAN calculations), indicating similar sensitivity to background conditions. Pearson correlation coefficients for window 4 is 4.5%, while there is no change in window 3. The $\sigma_{inter-window}$ values show variation, with the TCCON database showing a 6% difference between perturbed and non-perturbed cases. For the biases w.r.t. the TCCON database, window 2 shows the most sensitivity, with a 16% and 2.6% difference for HITRAN and GEISA. In summary the results from this analysis suggest the inter-window and inter-database biases identified in section 3.3 are variable depending on the uncertaintyassociated with the a priori and parameter information. Methane profile shape and pressure profile errors are especially significant, but in all cases the errors effect different bands in different databases differently, with windows 2 and generally indicate lower levels of sensitivity to variations of local conditions than window 1, suggesting the spectroscopic parameters for $^{13}CH_4$ in window 4 being particularly sensitive to errors. In addition the local conditions have an impact, with biases varying depending on the TCCON site and season. have significant uncertainty. Further to this, we found that the retrieval errors generated from $^{13}CH_4$ in window 4 were at least double those from $^{13}CH_4$ in window 1. This lower uncertainty is key in explaining the lower variation in $\delta^{13}C$ metric calculated using window 1.

An assessment of the sensitivity of Overall the results in Table 5 suggest using GEISA2020 $^{13}CH_4$ to errors in the a priori and parameter profiles is also included in Appendix C , generally indicating high sensitivity to all error sources. Windows 5 and 6 vary in their sensitivity, with the different spectroscopic databases showing similar sensitivity in window 5, but very different ones in window 6. retrievals from window 1 to calculate $\delta^{13}C$ values, showing high levels of consistency across all windows and sites, and relatively low bias levels. This consistency is surprising and is worth further investigation, however, Window 4 for all spectroscopic databases yield far less accurate results, suggesting more work must be done for spectroscopic parameters in this window for $^{13}CH_4$.

4 Discussion

We ~~find significant variations in retrieved DMFs across all of the considered windows and spectroscopic databases in this study, are most likely due to imperfections in the spectroscopic parameters. The results identify that each database reacts differently to a priori and parameter uncertainty, as well as variability in local conditions~~ have shown the presence of correlations between variations in specific local conditions and retrieval biases in this paper, however it should be noted that other local conditions do vary in parallel with those indicated in Sect. 3.3. It is ~~difficult to attribute the biases we have identified to specific spectroscopic parameters errors,~~ therefore likely that each window and spectroscopic database show bias variability due to the ~~range of parameters used, and it is beyond the scope of this paper to do so.~~

~~In addition to differences between the spectroscopic databases, we have shown that there are significant differences between the spectral windows used for retrieving methane isotopologues. This would not be not a significant problem if the systematic biases between the windows were constant. However, we have shown that retrieval results from each window responds differently to uncertainty in the a priori and parameter profiles. We conclude that there is likely to be an underlying bias in all TCCON data that varies from retrieval to retrieval, and day to day~~variation of a number of conditions simultaneously, which is why each TCCON site shows different results. The key message remains true however, that different windows in different spectroscopic databases are sensitive to varying degrees to local changing conditions. Further analysis in this topic should be assessed, for example the impact of the air-mass factor changes or variations in the O_2 retrievals may be important. We note Cygan et al. (2012); Ngo et al. (2013) identify Voigt broadening parameters for O_2 as insufficient. The release of the GGG2020 environment may allow for the testing of the impact of non-Voigt parameters on O_2 retrievals. We have also not considered errors in the instruments themselves, for example variations in the instrument line shape function between different TCCON instruments could cause additional biases.

We note that advancements are currently being tested on retrievals of methane from TCCON spectra, for example with the "SFIT4" algorithm (Zhou et al., 2019), which allows for profile retrievals and would therefore ~~not be~~ be less subject to the methane profile errors ~~investigated in this study. The next generation of~~ that can occur in GGG retrievals (Wunch et al., 2011). In addition to profile retrievals, this study used the GGG2014 ~~, the so called "~~retrieval software, while the more recent version of this software GGG2020 ~~"~~ has also recently been released. This update includes an improved spectroscopic database (this database was used in this study, wrapped in the GGG2014 software) and the ability to use non-Voigt line shapes for methane. Therefore ~~the updates to GGG~~ further analysis using the GGG2020 software and the use of other algorithms in this study could yield improved or different results. However, it is likely that the bias problems identified in this study may remain to some degree.

In addition to understanding the biases associated with retrieving $^{12}CH_4$ DMFs from TCCON spectra with differing spectroscopic databases, this study touches a question that is of some interest to the community, “can we calculate realistic and constant $\delta^{13}C$ values from TCCON”. The results ~~from this study~~ shown in Table 5 suggest not this is not yet possible, ~~based on the results shown in Table 7 and given that the~~ since they are often significantly different from the tropospheric average $\delta^{13}C$ value which is assumed to be -47‰ (Sherwood et al., 2016), and ~~our results are significantly different from this.We~~

~~expect that large deviations from this value is unlikely,~~ variable between databases and windows. There are some interesting cases where results close to the expected δ^{13}C value are calculated (e.g. windows 1 & 1 for HITRAN at Tsukuba), however given the same database in the same windows yields a completely inaccurate result at another TCCON site, it is challenging to draw any conclusions without further analysis. What is clear however, is that the δ^{13}C values calculate using $^{13}CH_4$ retrievals from window 1 tend to have less biases than those calculated using window 4, and show less variation between windows and TCCON sites, as well as more consistent results between the spectroscopic databases. The implication of these results are that window 1 is superior to window 4 for retrieving $^{13}CH_4$ DMF, however whether this is due to superior information content, or more accurate knowledge of spectroscopic parameters requires further research.

However, given that TCCON retrieves total column estimates, and not in-situ samples ~~. This~~ as assumed by Sherwood et al. (2016) , this assumption of -47‰ is a little unfair, since this is an assumption based on lower tropospheric averages, and does not take into account sink processes that occur further up into the atmosphere. For example Rigby et al. (2017) assume a -2.6‰ fractionation due to the chlorine sink in the stratosphere, and significant fractionation does occur in the troposphere with the OH sink (Röckmann et al., 2011). However, it can be argued here that the priority in calculating an accurate value of δ^{13}C from TCCON is a full assessment of all of the systematic biases present in the retrievals, most notably the spectroscopic biases, before discussion of the true δ^{13}C value of the total column.

5 Conclusions

In this study, using the GGG2014 retrieval environment we retrieve $^{12}CH_4$ DMFs from ~~two TCCON sites~~ four TCCON sites over the course of a year in each case, with the aim of understanding the biases associated with retrieving methane ~~isotopologues~~ in the TROPOMI spectral region as opposed to standard TCCON methane windows. Four different windows covering the spectral range of the future S5/UVNS instrument and the current S5P/TROPOMI instrument are used. Three of the windows are routinely used in TCCON products, but the TROPOMI/UVNS window in the 4190-4340 cm^{-1} range is not. We use ~~four~~ five sources of spectroscopic parameters, the HITRAN2016, ~~GEISA2015~~GEISA2020, SEOM-IAS and internal TCCON ~~database~~ databases (GGG2014 and GGG2020) in order to assess the impact of spectroscopic database uncertainties. ~~Measurements are taken from two TCCON sites (Tsukuba, and Ascension island) to provide a range in atmospheric conditions.~~

~~We found that the SEOM-IAS and internal TCCON spectroscopy databases (with the SEOM-IAS database limited to window 1/4190-4340 cm^{-1} spectral range) showed the lowest biases and errors. The SEOM-IAS~~ Firstly we analysied the quality of fit of each of the windows for each of the spectroscopic databases, for each window we find the GGG2020 spectroscopic database shows the best fit metrics, ~~the most consistent retrievals, and the lowest sensitivity to a priori and parameter errors.~~

~~We find significant levels of bias between the retrieved $^{12}CH_4$ DMFs both~~ except in window 1, where the SEOM-IAS database has the best quality of fit. We note that while each TCCON site shows different fit statistics for each window, the order of the spectroscopic databases in terms of ~~spectral window and spectroscopic database. In some cases, similar~~

windows from different spectroscopic databases differ by as much as 50 ppb, which is much larger than the precision and accuracy requirements of TROPOMI. These biases remain consistent between TCCON sites, implying systematic errors in the spectroscopic parameters. quality of fit remains the same in all cases, with GGG2020 showing the best, followed by GGG2014, HITRAN2016 and GEISA2020. Window 1 (4190-4340 cm^{-1}) shows the lowest variation between the databases, typically < 10 ppb, and the short window 3 (6002 cm^{-1}) shows the most variation, typically > 20 ppb. shows the poorest quality fit of all of the windows, indicating room to improve the spectroscopic parameters for window 1.

The sensitivity of the retrieved $^{12}CH_4$ DMFs to locally changing conditions such as water vapour and to uncertainty in the a priori and parameter profiles is investigated.We find that Window 1 from the SEOM-IAS database is the most insensitive to these errors, while windows 2 Using metrics based on bias w.r.t the standard TCCON methane retrieval window (a weighted average of three windows), we found that each of the TCCON sites, the GGG2014 and 4 are the most sensitive.

The analysis in this study led to two key conclusions, firstly we recommend including the TROPOMI SWIR spectral region (in this study, window GGG2020 databases exhibited normalised biases <1) into future TCCON methane retrievals, due to the consistency of the retrievals presented in this study, and the consistency of the retrievals in the face of sensitivity errors. Secondly, based on major deviations between retrievals from different spectroscopic databases, and the differing sensitivities of spectroscopic databases and windowsto sensitivity errors, we call for further investigation into how to incorporate these errors into future satellite and TCCON retrievals.

$^{13}CH_4$ DMFs are also retrieved in parallel to $^{12}CH_4$, but are found to be too in-accurate for the communities needs. It was argued that the static nature of TCCON sites could reduce the high precision errors over a long period, however fundamental accuracy issues in the spectroscopic databases must be overcome first.

6 Transmission

Example transmission for Ascension Island.

Retrieval fit statistics for example Ascension Island retrieval in October 2016. The RMSE for each spectroscopic database is shown in row 1, with the results for windows 1-4 indicated in columns 1-4. The χ^2 values are shown in row 2 for each window. Window in the standard TCCON windows, meaning that these biases were below the retrieval noise limit and were therefore not significant. However in window 1

Window 1	Window 2	Window 3	Window 4
RMSE	TCCON: $8.748\text{x}10^{-3}$ HITRAN: $1.061\text{x}10^{-2}$ GEISA: $9.880\text{x}10^{-3}$	TCCON: $6.488\text{x}10^{-3}$ HITRAN: $7.035\text{x}10^{-3}$ GEISA: $7.296\text{x}10^{-3}$	
	SEOM: $8.508\text{x}10^{-3}$	SEOM: nan	
	TCCON: $6.482\text{x}10^{-3}$ HITRAN: $8.738\text{x}10^{-3}$ GEISA: $8.887\text{x}10^{-3}$	TCCON: $6.253\text{x}10^{-3}$ HITRAN: $6.723\text{x}10^{-3}$ GEISA: $6.906\text{x}10^{-3}$	
χ^2	TCCON: 1.524 HITRAN: 2.241 GEISA: 1.944	TCCON: 0.648 HITRAN: 0.762 GEISA: 0.820	TCCON: 0.0670 HITRAN: 0.112 GEISA: 0.116
	SEOM: 1.441	SEOM: nan	SEOM: nan

TCCON: 0.716
HITRAN: 0.828
GEISA: 0.874
SEOM: nan

Concerning the differences in fit quality between the Tsukuba and the Ascension Island TCCON instruments: both instruments run according to TCCON specifications but their respective configurations are not exactly the same. This is normal and necessary as different sites need local adjustments to account for different local conditions such as altitude, humidity or cloud

conditions. Most of the effects caused by such individual configurations are removed by the differential CO_2 and CH_4 DMF retrievals but will affect individual spectra.

In the case of Tsukuba and Ascension, the configuration effects cannot be compared directly except for detector noise, which turned out to be comparable. However , the signal on the detector of the Ascension Island instrument is at least 50% lower than that of the Tsukuba instrument.

Likely reasons are:

1) The Ascension FTS runs on a higher spectral resolution (0.014 cm^{-1} vs. 0.02 cm^{-1}) and a faster scanner speed (10 kHz vs. 7.5 kHz). Both reduce integration time per spectral pixel.

2) The illumination of the InGaAS detector on Ascension is kept low on purpose to avoid saturation. This setting cannot be readjusted in between site visits and has to last for months.

3) The solar tracker has known issues with pointing at the centre of the sun at low SZAs but cannot be replaced easily. In addition, dust buildup on the solar tracker mirrors reduces the reflectivity of the mirrors quickly. They are cleaned weekly but a signal loss in the order of 20% over a few days is not uncommon.

6 Retrieval statistics

Statistics for 40 retrievals from Tsukuba on 07/07/2016 based on metrics identified in retrieval abundances subsection of section 2.2. The first row indicates the standard deviation of the retrieved DMFs from each window under study in this paper (σ_{window}), with the target indicated for each window. The second data row indicates the standard deviation of the retrieved abundances of $^{12}CH_4$ for all windows present in each spectroscopic database ($\sigma_{inter-window}$), the third data row is as the second row, but for $^{13}CH_4$. The fourth to ninth data rows indicate the retrieved mean of the DMF for each window against the retrieved mean of the equivalent window using the TCCON spectroscopic database (bias), with the window in question indicated in the rows, and the spectroscopic database indicated in the columns. Window 1 ($^{12}CH_4$) 2 ($^{12}CH_4$) 3 ($^{12}CH_4$) 4 ($^{12}CH_4$) 5 ($^{13}CH_4$) 6 ($^{13}CH_4$) σ_{window} (ppb) 9.42 15.7 23.7 18.5 0.26 4.14 TCCON HITRAN GEISA SEOM-IAS 16.4 18.1 10.5 N/A 2.40 4.63 N/A N/A Database bias (ppb; , both GGG2014 and GGG2020 indicated biases >1 for most of the TCCON sites, suggesting TCCON retrievals in window 1) bias (ppb; window 2) bias (ppb; window 3) bias (ppb; window 4) bias (ppb; window 5) bias (ppb; window 6)

Statistics for 243 retrievals from Ascension Island on 23/08/2016 based on metrics identified in retrieval abundances subsection of section 2.2. The first row indicates the standard deviation of the retrieved DMFs from each window under study in this paper (σ_{window}), with the target indicated for each window. The second data row indicates the standard deviation of the retrieved abundances of $^{12}CH_4$ for all windows present in each spectroscopic database ($\sigma_{inter-window}$), the third data row is as the second row, but for $^{13}CH_4$. The fourth to ninth data rows indicate the retrieved mean of the DMF for each window against the retrieved mean of the equivalent window using the TCCON spectroscopic database (bias), with the window in question highlighted in the rows, and the spectroscopic database indicated in the columns. Window 1 ($^{12}CH_4$) 2 ($^{12}CH_4$) 3 ($^{12}CH_4$) 4 ($^{12}CH_4$) 5 ($^{13}CH_4$) 6 ($^{13}CH_4$) σ_{window} (ppb) 10.0 18.3 23.2 17.9 1.02 3.22 TCCON have a significant bias to the standard

TCCON window. Similarly the HITRAN ~~GEISA SEOM-IAS 16.4 18.1 13.4 N/A 1.69 1.99 N/A N/A Database bias (ppb; window1) bias (ppb; window~~ and GEISA databases showed significant biases (in some cases >2) ~~bias (ppb; window 3) bias (ppb; window 4) bias (ppb; window 5) bias (ppb; window 6)~~

6 ~~Sensitivity errors~~

5.1 ~~Methane Profile shift~~

~~An analysis on the impact of inserting a 2% methane profile shift error into the a priori information is included in this sub-appendix. Table C1 below allows for direct comparison with Table 5 of the impact of this shift.~~

~~Statistics as Table 5 for the methane profile shift case identified in sect. 2.4. Data is for April 2016 Tsukuba retrievals. Window~~ w.r.t the standard in windows 1 ~~($^{12}CH_4$) 2 ($^{12}CH_4$) 3 ($^{12}CH_4$)~~ and 4~~($^{12}CH_4$) 5 ($^{13}CH_4$) 6 ($^{13}CH_4$) σ_{window} (ppb) 9.03 17.6 22.5 12.9 0.591 1.65 TCCON HITRAN GEISA SEOM-IAS 16.5 19.9 9.32 N/A 1.09 0.388 N/A N/A Database bias (ppb; window 1) bias (ppb; window~~ , indicating significant disagreement between the standard TCCON retrievals and the HITRAN and GEISA databases in these windows. Only the GEISA database showed significant disagreement with the standard in windows 2 ~~) bias (ppb; window 3) bias (ppb; window 4) bias (ppb; window 5) bias (ppb; window 6)~~ & 3, which, based on the other results shown in this paper, suggest the GEISA database as having the largest differences of all of the databases considered in this study.

~~Further analysis is below, showing the linear relationship between the original standard retrievals, and the perturbed retrievals.All Tsukuba and Ascension island retrievals considered in this study are included in these figures.~~

~~Series of scatter plots showing unperturbed retrieved DMFs $^{12}CH_4$ and $^{13}CH_4$ from the cases indicated in sect. 3.3 and Appendix B, against these cases when perturbed by a 2% shift to the a priori methane profile. Each column indicates the window under consideration, the top row is for Tsukuba data (TK), and the bottom row is for Ascension Island data (AI). The colours in the plots are consistent with the rest of this paper in indicating the spectroscopic database. The units for all axes are indicated in the titles.~~

~~Figure C1 qualitatively indicates some sensitivity to methane profile perturbation, the linear regression statistics of Fig. C1 are shown in Fig C2, including slope, intercept, coefficient of determination and standard deviation.~~

~~Plot indicating the linear statistical relationship between the perturbed and unperturbed $^{12}CH_4$ and $^{13}CH_4$ DMFs indicated in Fig C1. The x-axis for all plots indicates the retrieval window under consideration. The first column shows the values for the linear slope, the second column is the linear intercept, the third column is the coefficient of determination and the fourth column is the standard deviation. The first row indicates retrievals from Tsukuba and the second row shows retrievals from Ascension island. The colours in the plots are consistent with the rest of this paper in indicating the spectroscopic database.~~

~~Figure C2 builds on the quantification in Table C1, and shows low dependency on errors in a methane profile shift, with no clear patterns between windows and spectroscopic databases.~~

5.1 Methane Profile Shape

An analysis on the impact of inserting a methane profile shape error into the a priori information is included in this sub-appendix. The retrievals from Tsukuba April 2016 use the methane profile of Tsukuba July 2016 and vice versa, and the retrievals from Ascension island August 2016 use the methane profile of Ascension island October 2016 and vice versa. Table C2 below allows for direct comparison with Table 5 of the impact of this shift.

Statistics as Table 5 for the methane profile shape change case identified in sect. 2.4. Data is for April 2016 Tsukuba retrievals. Window 1 (The sensitivity of the retrieved $^{12}CH_4$) 2 ($^{12}CH_4$) 3 ($^{12}CH_4$) 4 ($^{12}CH_4$) 5 ($^{13}CH_4$) 6 ($^{13}CH_4$) σ_{window} (ppb) 8.98 19.12 23.6 13.02 0.569 1.63 TCCON HITRAN GEISA SEOM-IAS 17.7 21.1 9.15 N/A 1.11 0.409 N/A N/A Database bias (ppb; window 1) bias (ppb; window 2) bias (ppb; window 3) bias (ppb; window 4) bias (ppb; window 5) bias (ppb; window 6)

Further analysis is below, showing the linear relationship between the original standard retrievals, and the perturbed retrievals. All Tsukuba and Ascension island retrievals considered in this study are included in these figures.

Series of scatter plots showing unperturbed retrieved DMFs $^{12}CH_4$ and $^{13}CH_4$ from the cases indicated in sect. 3.3 and Appendix B, against these cases when perturbed by a change to the a priori methane profile. Each column indicates the window under consideration, the top row is for Tsukuba data (TK), and the bottom row is for Ascension Island data (AI). The colours in the plots are consistent with the rest of this paper in indicating the spectroscopic database. The units for all axes are indicated in the titles.

Fig C3 qualitatively indicates significant sensitivity to a methane profile shape perturbation, the linear regression statistics of Fig. C3 are shown in Fig C4, including slope, intercept, coefficient of determination and standard deviation.

Plot indicating the linear statistical relationship between the perturbed and unperturbed $^{12}CH_4$ and $^{13}CH_4$ DMFs indicated in Fig C3 for the methane profile shape case. The x-axis for all plots indicates the retrieval window under consideration. The first column shows the values for the linear slope, the second column is the linear intercept, the third column is the coefficient of determination and the fourth column is the standard deviation. The first row indicates retrievals from Tsukuba and the second row shows retrievals from Ascension island. The colours in the plots are consistent with the rest of this paper in indicating the spectroscopic database.

Figure C4 indicates that Tsukuba retrievals were more sensitive to a change in profile shape than Ascension island, most likely because there is a more significant shift in the Tsukuba spring-summer profile, as opposed to the summer-autumn profile for Ascension island, where there are no seasons. Interestingly the HITRAN2016 retrievals are the most affected in the Tsukuba case, but there is no such clear pattern in Ascension island. Based on the results in Fig C4, we can assume that the magnitude of the biases specified in Table C2 will be as large (if not larger) for the Tsukuba July 2016 case, but no more significant than the results shown in Table C1 for the Ascension island cases.

5.1 Water Vapour

An analysis on the impact of inserting a 10% water vapour profile shift error into the a priori information is included in this sub-appendix. Table C3 below allows for direct comparison with Table 5 of the impact of this shift.

Statistics as Table 5 for the water profile profile shift case identified in sect. 2.4. Data is for April 2016 Tsukuba retrievals. Window 1 ($^{12}CH_4$) 2 ($^{12}CH_4$) 3 ($^{12}CH_4$) 4 ($^{12}CH_4$) 5 ($^{13}CH_4$) 6 ($^{13}CH_4$) σ_{window} (ppb) 9.02 17.4 22.5 12.9 0.556 1.65 TCCON HITRAN GEISA SEOM-IAS 16.5 20.0 9.15 N/A 1.09 0.406 N/A N/A Database bias (ppb; window 1) bias (ppb; window 2) bias (ppb; window 3) bias (ppb; window 4) bias (ppb; window 5) bias (ppb; window 6)

Further analysis is below, showing the linear relationship between the original standard retrievals, and the perturbed retrievals. All Tsukuba and Ascension island retrievals considered in this study are included in these figures.

Series of scatter plots showing unperturbed retrieved DMFs $^{12}CH_4$ and $^{13}CH_4$ from the cases indicated in sect. 3.3 and Appendix B, against these cases when perturbed by a change to the a priori water vapour profile. Each column indicates the window under consideration, the top row is for Tsukuba data (TK), and the bottom row is for Ascension Island data (AI). The colours in the plots are consistent with the rest of this paper in indicating the spectroscopic database. The units for all axes are indicated in the titles.

Figure C5 shows that Tsukuba is far more sensitive to errors in the a priori water vapour column in some spectral windows than Ascension island. We note that the conditions for Tsukuba site in July of 2016 (indicated in Table D1) show very high levels of DMFs to locally changing conditions such as water vapour, which is a possible cause for this apparent sensitivity. The linear regression statistics shown in Fig. C6 below explore these differences in more detail.

Plot indicating the linear statistical relationship between the perturbed and unperturbed $^{12}CH_4$ and $^{13}CH_4$ DMFs indicated in Fig C3 for the water vapour profile shift case. The x-axis for all plots indicates the retrieval window under consideration. The first column shows the values for the linear slope, the second column is the linear intercept, the third column is the coefficient of determination and the fourth column is the standard deviation. The first row indicates retrievals from Tsukuba and the second row shows retrievals from Ascension island. The colours in the plots are consistent with the rest of this paper in indicating the spectroscopic database.

Figure C6 shows some significant sensitivities to water vapour uncertainty, especially for retrievals from Tsukuba in window 2 for all spectroscopic databases, where the intercept value of 2.5 ppm is many times higher than any of the other cases shown in Fig. C6. We note that the values indicated in Table C3 are not significantly different from those in Table 5, suggesting that the majority of the errors occur in the July Tsukuba retrievals. The statistics for the Ascension island retrievals show similar values to those for the methane profile shift sensitivities, shown in Fig. C2, indicating lower sensitivity to water vapour uncertainty. Ascension island retains a consistent year round humidity due to its location; conversely Tsukuba has a wide range of seasons and therefore highly variable humidity, indicated in Table D1. The implication of these results is that a priori water vapour uncertainty only has a significant impact in high humidity environments.

5.1 Pressure

An analysis on the impact of inserting a 2% pressure profile shift error into the parameter information is included in this sub-appendix. Table C4 below allows for direct comparison with Table 5 of the impact of this shift.

Statistics as Table 5 for the pressure profile shift case identified in sect. 2.4. Data is for April 2016 Tsukuba retrievals. Window 1 ($^{12}CH_4$) 2 ($^{12}CH_4$) 3 ($^{12}CH_4$) 4 ($^{12}CH_4$) 5 ($^{13}CH_4$) 6 ($^{13}CH_4$) σ_{window} (ppb) 9.02 17.64 22.7 12.9 0.593 1.69 TCCON HITRAN GEISA SEOM-IAS 15.1 18.5 10.7 N/A 1.10 0.383 N/A N/A Database bias (ppb; window 1) bias (ppb; window 2) bias (ppb; window 3) bias (ppb; window 4) bias (ppb; window 5) bias (ppb; window 6)

Further analysis is below, showing the linear relationship between the original standard retrievals, and the perturbed retrievals for all retrievals considered in this studySZA and temperature is investigated. We find significant levels of dependence on these variations that are not necessarily mirrored across all of the TCCON sites. We conclude that some retrieval windows and spectroscopic databases are more sensitive to variable conditions than others. This sensitivity is exacerbated at TCCON locations with highly variable and challenging local conditions.

Series of scatter plots indicating the differences between retrieved values of $^{12}CH_4$ and $^{13}CH_4$ DMFs from the standard cases shown in sect. 3.3 and when a 2 % pressure shift is applied to the a priori atmosphere. Each column indicates the window under consideration, the top row is for Tsukuba data (TK), and the bottom row is for Ascension Island data (AI). The colours in the plots are consistent with the rest of this paper in indicating the spectroscopic database.

The results shown in Fig. C7 qualitatively indicate that there is significant dependency on the accurate knowledge of the pressure profile, which varies between the TCCON sites.Figure C8 below quantitatively explores the variations though linear regression statistics.

Plot indicating the linear statistical relationship between the standard retrievals from sect 3.3 and the perturbed pressure column retrievals. The x-axis for all plots indicates the retrieval window under consideration. The first column shows the values for the linear slope, the second column is the linear intercept, the third column is the coefficient of determination and the fourth column is the standard deviation. The first row indicates retrievals from Tsukuba and the second row shows retrievals from Ascension island. The colours in the plots are consistent with the rest of this paper in indicating the spectroscopic database.

Figure C8 shows that the sensitivity of retrieved $^{12}CH_4$ The δ^{13}C metric calculated in this study show significant bias w.r.t the expected total column value of -47‰. However, the use of the 4265 cm^{-1} window shows significant benefit over the 6076 cm^{-1} window, and $^{13}CH_4$ DMFs to a systematic bias in the pressure profile varies depending on the spectroscopic database, and the window. The fact that different spectroscopic databases and different windows react differently to pressure profile error is not surprising, the significance of the differences in all cases is. For the $^{12}CH_4$ cases (windows 1-4), window 2 typically shows the most sensitivity while for the $^{13}CH_4$ cases (windows 5-6), window6 shows the most sensitivity. Interestingly, the results from Ascension island suggest greater insensitivity to the pressure error, but this could be attributed to a greater number of measurements available for this analysis. Comparisons of Table C4 with Tables C2 and 5 suggest the pressure column error has a greater impact on the bias against TCCON database retrievals, but the overall window and inter-window deviation is more significant with methane profile shape errorsmore consistent results across spectroscopic databases.

5.1 Temperature

An analysis on the impact of inserting a 2 K temperature profile shift error into the parameter information is included in this sub-appendix. Table C5 below allows for direct comparison with Table 5 of the impact of this shift.

Statistics as Table 5 for the temperature profile shift case identified in sect. 2.4. Data is for April 2016 Tsukuba retrievals. Window 1 ($^{12}CH_4$) 2 ($^{12}CH_4$) 3 ($^{12}CH_4$) 4 ($^{12}CH_4$) 5 ($^{13}CH_4$) 6 ($^{13}CH_4$) σ_{window} (ppb) 9.05 17.8 22.5 13.2 0.634 1.62 TCCON HITRAN GEISA SEOM-IAS 17.5 20.8 8.4 N/A 0.539 0.442 N/A N/A Database bias (ppb; window 1) bias (ppb; window 2) bias (ppb; window 3) bias (ppb; window 4) bias (ppb; window 5) bias (ppb; window 6)

Further analysis is below, showing the linear relationship between the original standard retrievals, and the perturbed retrievals for all retrievals considered The analysis in this study led to two key conclusions, firstly we recommend including the TROPOMI SWIR spectral region (in this study, window 1) into future TCCON methane retrievals. This is based on comparable fit statistics with the original TCCON methane windows, and the significant bias w.r.t the standard TCCON retrieval product. Secondly, the different spectral windows used to generate the TCCON methane products are affected by local condition variability to varying degrees. Suggesting the weighted average normally used to generate TCCON methane products should be a unique formation depending on TCCON site and season.

Series of scatter plots indicating the differences between retrieved values of $^{12}CH_4$ and $^{13}CH_4$ DMFs from the standard cases shown in sect. 3.3 and when a 2 K temperature shift is applied to the a priori atmosphere. Each column indicates the window under consideration, the top row is for Tsukuba data (TK), and the bottom row is for Ascension Island data (AI). The colours in the plots are consistent with the rest of this paper in indicating the spectroscopic database.

Figure C9 qualitatively shows adding a 2 K temperature bias into the parameter profile has a notable impact on the retrievalsof $^{12}CH_4$ and $^{13}CH_4$ DMFs, especially windows 2 and 6. This is explored quantitatively in Figure C10.

Code and data availability. The GGG2014 retrieval environment is available at https://tccon-wiki.caltech.edu, and TCCON L1b spectra are available upon discussion with the relevant site PI

Plot indicating the linear statistical relationship between the standard retrievals from sect 3.3 and the perturbed temperature column retrievals. The x-axis for all plots indicates the retrieval window under consideration. The first column shows the values for the linear slope, the second column is the linear intercept, the third column is the coefficient of determination and the fourth column is the standard deviation. The first row indicates retrievals from Tsukuba and the second row shows retrievals from Ascension island. The colours in the plots are consistent with the rest of this paper in indicating the spectroscopic database.

The statistics indicated in Fig. C10 show a significant sensitivity to temperature biases, particularly at Tsukuba. Windows 2 and 4 show the most sensitivity in $^{12}CH_4$ DMFs, and window 6 shows the most for $^{13}CH_4$ DMFs. There is limited deviation between the spectroscopic databases in terms of sensitivity for each window, except for window 4 which shows more variability in this regards. The scale of these statistics is not as significant as those indicated in Figs C4 and C8 for methane profile and pressure profile errors respectively.Comparing the results from Table C5 with Table C4 and Table 5, it is possible to see that window deviation is similar in all cases, but the inter-window deviation is larger in the pressure profile errors case, but the biases tend to be larger in the temperature error case. Figures C7 and C8 seem to suggest larger errors for Ascension island than in Figures C9 and C10. These results suggest that retrievals of $^{12}CH_4$ DMFs and especially $^{13}CH_4$ DMFs are sensitive to temperature errors, and they depend on location and seasonsignificantly.

6 ~~Additional data~~

~~Daily ranges of a priori and measured surface temperatures, and averaged H_2O DMFs from both TCCON sites.~~

Site	measured temperature (°C)	a priori surface temperature (°C)	H_2O (average)	standard deviation	SZA range (°)
Tsukuba (01/April/2016)	12.0	15.8-16.8	2069 ppm	47 ppm	34-43
Tsukuba (01/July/2016)	25.1	29.2-33.2	6896 ppm	70 ppm	13-26
Ascension Island (23/Aug/2016)	22.4	24-27.3	3752 ppm	91 ppm	19-81
Ascension Island (01/Oct/2016)	22	24.3-25.9	4345 ppm	83 ppm	7-75

~~Water vapour retrievals are taken from the 4565 cm^{-1} spectral window.~~

Author contributions. MB provided and processed the Ny-Ålesund data, ND provided and processed the Darwin data, DGF provided and processed the Ascension Island TCCON data and IM provided and processed the Tsukuba TCCON data. EM devised and performed the study, analysed the data and wrote the paper. BV consulted on the interpretation of the results. All authors reviewed the paper.

Competing interests. BV is an associate editor for the joint (AMT/ACP) special issue "TROPOMI on Sentinel-5 Precursor: first year in operation". DGF is an associate editor for AMT.

Acknowledgements. This study has been performed in the framework of the postdoctoral Research Fellowship program of the European Space Agency (ESA). The GGG2014 retrieval environment was developed at the California institute of Technology (Caltech), and is available at https://tccon-wiki.caltech.edu. Thanks to Geoff Toon at Caltech for providing advice on the use of GGG2014. HITRAN2016 is available at https://hitran.org/, ~~GEISA2015~~ GEISA2020 is available from http://ara.abct.lmd.polytechnique.fr/index.php?page=geisa-2. The SEOM-IAS database is available at https://www.wdc.dlr.de/seom-ias/. The TCCON line ~~list is~~ lists are described in the GGG documentation. The Ascension Island TCCON station has been supported by ESA under grant 3-14737 and by the German Bundesministerium für Wirtschaft und Energie (BMWi) under grants 50EE1711C and 50EE1711E. We thankfully acknowledge funding from the University of Bremen and the German Research Foundation (DFG) – Projektnummer 268020496 – TRR 172 – (AC)3 and thank the AWIPEV station personnel in Ny-Ålesund and the Alfred-Wegener Institute Potsdam for their continuous support. The TCCON sites at Tsukuba is supported in part by the GOSAT series project. The Darwin TCCON station is funded by NASA grants NAG5- 12247 and NNG05-GD07G and supported by the Australian Research Council (ARC) grants DP1601001598, DP140101552, DP110103118, DP0879468 and LP0562346. Thanks to Anu Dudhia at Oxford University for the Fortran routine to convert the GEISA line structure into a HITRAN line structure.

References

Albert, S., Bauerecker, S., Boudon, V., Brown, L., Champion, J.-P., Loëte, M., Nikitin, A., and Quack, M.: Global analysis of the high resolution infrared spectrum of methane 12CH4 in the region from 0 to 4800cm-1, Chemical Physics, 356, 131–146, https://doi.org/10.1016/j.chemphys.2008.10.019, 2009.

An, X., Caswell, A. W., and Sanders, S. T.: Quantifying the temperature sensitivity of practical spectra using a new spectroscopic quantity: Frequency-dependent lower-state energy, Journal of Quantitative Spectroscopy and Radiative Transfer, 112, 779–785, https://doi.org/10.1016/j.jqsrt.2010.10.014, 2011.

Armante, R., Scott, N., Crevoisier, C., Capelle, V., Crepeau, L., Jacquinet, N., and Chédin, A.: Evaluation of spectroscopic databases through radiative transfer simulations compared to observations. Application to the validation of GEISA 2015 with IASI and TCCON, Journal of Molecular Spectroscopy, 327, 180–192, https://doi.org/10.1016/j.jms.2016.04.004, 2016.

Bernath, P. F., McElroy, C. T., Abrams, M. C., Boone, C. D., Butler, M., Camy-Peyret, C., Carleer, M., Clerbaux, C., Coheur, P., Colin, R., DeCola, P., DeMazière, M., Drummond, J. R., Dufour, D., Evans, W. F. J., Fast, H., Fussen, D., Gilbert, K., Jennings, D. E., Llewellyn, E. J., Lowe, R. P., Mahieu, E., McConnell, J. C., McHugh, M., McLeod, S. D., Michaud, R., Midwinter, C., Nassar, R., Nichitiu, F., Nowlan, C., Rinsland, C. P., Rochon, Y. J., Rowlands, N., Semeniuk, K., Simon, P., Skelton, R., Sloan, J. J., Soucy, M., Strong, K., Tremblay, P., Turnbull, D., Walker, K. A., Walkty, I., Wardle, D. A., Wehrle, V., Zander, R., and Zou, J.: Atmospheric Chemistry Experiment (ACE): Mission overview, Geophysical Research Letters, 32, L15S01, https://doi.org/10.1029/2005GL022386, 2005.

Birk, M., Wagner, G., Loos, J., Mondelain, D., and Campargue, A.: ESA SEOM-IAS – Spectroscopic parameters database 2.3 μm region, https://doi.org/10.5281/ZENODO.1009126, 2017.

Bovensmann, H., Burrows, J. P., Buchwitz, M., Frerick, J., Noël, S., Rozanov, V. V., Chance, K. V., and Goede, A. P. H.: SCIAMACHY: Mission Objectives and Measurement Modes, Journal of the Atmospheric Sciences, 56, 127–150, https://doi.org/10.1175/1520-0469(1999)056<0127:SMOAMM>2.0.CO;2, 1999.

Brown, L. R., Sung, K., Benner, D. C., Devi, V. M., Boudon, V., Gabard, T., Wenger, C., Campargue, A., Leshchishina, O., Kassi, S., Mondelain, D., Wang, L., Daumont, L., Régalia, L., Rey, M., Thomas, X., Tyuterev, V. G., Lyulin, O. M., Nikitin, A. V., Niederer, H. M., Albert, S., Bauerecker, S., Quack, M., O'Brien, J. J., Gordon, I. E., Rothman, L. S., Sasada, H., Coustenis, A., Smith, M. A., Carrington, T., Wang, X. G., Mantz, A. W., and Spickler, P. T.: Methane line parameters in the HITRAN2012 database, Journal of Quantitative Spectroscopy and Radiative Transfer, 130, 201–219, https://doi.org/10.1016/j.jqsrt.2013.06.020, 2013.

Buzan, E. M., Beale, C. A., Boone, C. D., and Bernath, P. F.: Global stratospheric measurements of the isotopologues of methane from the Atmospheric Chemistry Experiment Fourier transform spectrometer, Atmos. Meas. Tech, 9, 1095–1111, https://doi.org/10.5194/amt-9-1095-2016, 2016.

Checa-Garcia, R., Landgraf, J., Galli, A., Hase, F., Velazco, V. A., Tran, H., Boudon, V., Alkemade, F., and Butz, A.: Mapping spectroscopic uncertainties into prospective methane retrieval errors from Sentinel-5 and its precursor, Atmospheric Measurement Techniques, 8, 3617–3629, https://doi.org/10.5194/amt-8-3617-2015, 2015.

Crisp, D., Fisher, B. M., O 'dell, C., Frankenberg, C., Basilio, R., Bösch, H., Brown, L. R., Castano, R., Connor, B., Deutscher, N. M., Eldering, A., Griffith, D., Gunson, M., Kuze, A., Mandrake, L., Mcduffie, J., Messerschmidt, J., Miller, C. E., Morino, I., Natraj, V., Notholt, J., O 'brien, D. M., Oyafuso, F., Polonsky, I., Robinson, J., Salawitch, R., Sherlock, V., Smyth, M., Suto, H., Taylor, T. E., Thompson, D. R., Wennberg, P. O., Wunch, D., and Yung, Y. L.: The ACOS CO 2 retrieval algorithm – Part II: Global X CO 2 data characterization, Atmos. Meas. Tech, 5, 687–707, https://doi.org/10.5194/amt-5-687-2012, 2012.

Cygan, A., Lisak, D., Wójtewicz, S., Domysławska, J., Hodges, J. T., Trawiński, R. S., and Ciuryło, R.: High-signal-to-noise-ratio laser technique for accurate measurements of spectral line parameters, Physical Review A - Atomic, Molecular, and Optical Physics, 85, 022 508, https://doi.org/10.1103/PhysRevA.85.022508, 2012.

Delahaye, T., Armante, R., Scott, N., Jacquinet-Husson, N., Chédin, A., Crépeau, L., Crevoisier, C., Douet, V., Perrin, A., Barbe, A., Boudon, V., Campargue, A., Coudert, L., Ebert, V., Flaud, J.-M., Gamache, R., Jacquemart, D., Jolly, A., Kwabia Tchana, F., Kyuberis, A., Li, G., Lyulin, O., Manceron, L., Mikhailenko, S., Moazzen-Ahmadi, N., Müller, H., Naumenko, O., Nikitin, A., Perevalov, V., Richard, C., Starikova, E., Tashkun, S., Tyuterev, V., Vander Auwera, J., Vispoel, B., Yachmenev, A., and Yurchenko, S.: The 2020 edition of the GEISA spectroscopic database, Journal of Molecular Spectroscopy, 380, 111 510, https://doi.org/10.1016/j.jms.2021.111510, 2021.

Drummond, J. R. and Mand, G. S.: The measurements of pollution in the troposphere (MOPITT) instrument: Overall performance and calibration requirements, Journal of Atmospheric and Oceanic Technology, 13, 314–320, https://doi.org/10.1175/1520-0426(1996)013<0314:TMOPIT>2.0.CO;2, 1996.

Fisher, R. E., France, J. L., Lowry, D., Lanoisellé, M., Brownlow, R., Pyle, J. A., Cain, M., Warwick, N., Skiba, U. M., Drewer, J., Dinsmore, K. J., Leeson, S. R., Bauguitte, S. J.-B., Wellpott, A., O'Shea, S. J., Allen, G., Gallagher, M. W., Pitt, J., Percival, C. J., Bower, K., George, C., Hayman, G. D., Aalto, T., Lohila, A., Aurela, M., Laurila, T., Crill, P. M., McCalley, C. K., and Nisbet, E. G.: Measurement of the 13C isotopic signature of methane emissions from northern European wetlands, Global Biogeochemical Cycles, 31, 605–623, https://doi.org/10.1002/2016GB005504, 2017.

Galli, A., Butz, A., Scheepmaker, R. A., Hasekamp, O., Landgraf, J., Tol, P., Wunch, D., Deutscher, N. M., Toon, G. C., Wennberg, P. O., Griffith, D. W., and AbenI.: CH4, CO, and H2O spectroscopy for the Sentinel-5 Precursor mission: An assessment with the Total Carbon Column Observing Network measurements, Atmospheric Measurement Techniques, 5, 1387–1398, https://doi.org/10.5194/amt-5-1387-2012, 2012.

Gordon, I., Rothman, L., Hill, C., Kochanov, R., Tan, Y., Bernath, P., Birk, M., Boudon, V., Campargue, A., Chance, K., Drouin, B., Flaud, J.-M., Gamache, R., Hodges, J., Jacquemart, D., Perevalov, V., Perrin, A., Shine, K., Smith, M.-A., Tennyson, J., Toon, G., Tran, H., Tyuterev, V., Barbe, A., Császár, A., Devi, V., Furtenbacher, T., Harrison, J., Hartmann, J.-M., Jolly, A., Johnson, T., Karman, T., Kleiner, I., Kyuberis, A., Loos, J., Lyulin, O., Massie, S., Mikhailenko, S., Moazzen-Ahmadi, N., Müller, H., Naumenko, O., Nikitin, A., Polyansky, O., Rey, M., Rotger, M., Sharpe, S., Sung, K., Starikova, E., Tashkun, S., Auwera, J. V., Wagner, G., Wilzewski, J., Wcisło, P., Yu, S., and Zak, E.: The HITRAN2016 Molecular Spectroscopic Database, Journal of Quantitative Spectroscopy and Radiative Transfer, https://doi.org/10.1016/j.jqsrt.2017.06.038, 2017.

Hu, H., Hasekamp, O., Butz, A., Galli, A., Landgraf, J., Aan De Brugh, J., Borsdorff, T., Scheepmaker, R., and Aben, I.: The operational methane retrieval algorithm for TROPOMI, Atmos. Meas. Tech, 9, 5423–5440, https://doi.org/10.5194/amt-9-5423-2016, 2016.

Ingmann, P., Veihelmann, B., Langen, J., Lamarre, D., Stark, H., and Courrèges-Lacoste, G. B.: Requirements for the GMES Atmosphere Service and ESA's implementation concept: Sentinels-4/-5 and -5p, Remote Sensing of Environment, 120, 58–69, https://doi.org/10.1016/J.RSE.2012.01.023, 2012.

IPCC: Fifth Assessment Report - Impacts, Adaptation and Vulnerability, http://www.ipcc.ch/report/ar5/wg2/, 2014.

Jacquinet-Husson, N., Armante, R., Scott, N. A., Chédin, A., Crépeau, L., Boutammine, C., Bouhdaoui, A., Crevoisier, C., Capelle, V., Boonne, C., Poulet-Crovisier, N., Barbe, A., Chris Benner, D., Boudon, V., Brown, L. R., Buldyreva, J., Campargue, A., Coudert, L. H., Devi, V. M., Down, M. J., Drouin, B. J., Fayt, A., Fittschen, C., Flaud, J. M., Gamache, R. R., Harrison, J. J., Hill, C., Hodnebrog, Hu, S. M., Jacquemart, D., Jolly, A., Jiménez, E., Lavrentieva, N. N., Liu, A. W., Lodi, L., Lyulin, O. M., Massie, S. T., Mikhailenko, S., Müller, H. S., Naumenko, O. V., Nikitin, A., Nielsen, C. J., Orphal, J., Perevalov, V. I., Perrin, A., Polovtseva, E., Predoi-Cross, A., Rotger, M.,

Ruth, A. A., Yu, S. S., Sung, K., Tashkun, S. A., Tennyson, J., Tyuterev, V. G., Vander Auwera, J., Voronin, B. A., and Makie, A.: The 2015 edition of the GEISA spectroscopic database, Journal of Molecular Spectroscopy, 327, 31–72, https://doi.org/10.1016/j.jms.2016.06.007, 2016.

Kirschke, S., Bousquet, P., Ciais, P., Saunois, M., Canadell, J. G., Dlugokencky, E. J., Bergamaschi, P., Bergmann, D., Blake, D. R., Bruhwiler, L., Cameron-Smith, P., Castaldi, S., Chevallier, F., Feng, L., Fraser, A., Heimann, M., Hodson, E. L., Houweling, S., Josse, B., Fraser, P. J., Krummel, P. B., Lamarque, J. F., Langenfelds, R. L., Le Quéré, C., Naik, V., O'doherty, S., Palmer, P. I., Pison, I., Plummer, D., Poulter, B., Prinn, R. G., Rigby, M., Ringeval, B., Santini, M., Schmidt, M., Shindell, D. T., Simpson, I. J., Spahni, R., Steele, L. P., Strode, S. A., Sudo, K., Szopa, S., Van Der Werf, G. R., Voulgarakis, A., Van Weele, M., Weiss, R. F., Williams, J. E., and Zeng, G.: Three decades of global methane sources and sinks, https://doi.org/10.1038/ngeo1955, 2013.

Kuze, A., Suto, H., Nakajima, M., and Hamazaki, T.: Thermal and near infrared sensor for carbon observation Fourier-transform spectrometer on the Greenhouse Gases Observing Satellite for greenhouse gases monitoring, Applied Optics, 48, 6716, https://doi.org/10.1364/AO.48.006716, 2009.

Laughner, J., Andrews, A., Roche, S., Kiel, M., and Toon, G.: ginput v1.0.10: GGG2020 prior profile software (Version 1.0.10), https://doi.org/10.22002/D1.1944, 2021.

Lorente, A., Borsdorff, T., Butz, A., Hasekamp, O., Aan De Brugh, J., Schneider, A., Wu, L., Hase, F., Kivi, R., Wunch, D., Pollard, D. F., Shiomi, K., Deutscher, N. M., Velazco, V. A., Roehl, C. M., Wennberg, P. O., Warneke, T., and Landgraf, J.: Methane retrieved from TROPOMI: Improvement of the data product and validation of the first 2 years of measurements, Atmospheric Measurement Techniques, 14, 665–684, https://doi.org/10.5194/amt-14-665-2021, 2021.

Malina, E., Yoshida, Y., Matsunaga, T., and Muller, J. P.: Information content analysis: The potential for methane isotopologue retrieval from GOSAT-2, Atmospheric Measurement Techniques, 11, 1159–1179, https://doi.org/10.5194/amt-11-1159-2018, 2018.

Malina, E., Hu, H., Landgraf, J., and Veihelmann, B.: A study of synthetic 13 CH 4 retrievals from TROPOMI and Sentinel-5/UVNS, Atmos. Meas. Tech, 12, 6273–6301, https://doi.org/10.5194/amt-12-6273-2019, 2019.

Mcnorton, J., Chipperfield, M. P., Gloor, M., Wilson, C., Feng, W., Hayman, G. D., Rigby, M., Krummel, P. B., O 'doherty, S., Prinn, R. G., Weiss, R. F., Young, D., Dlugokencky, E., and Montzka, S. A.: Role of OH variability in the stalling of the global atmospheric CH 4 growth rate from 1999 to 2006, Atmos. Chem. Phys, 16, 7943–7956, https://doi.org/10.5194/acp-16-7943-2016, 2016.

Mendonca, J., Strong, K., Sung, K., Devi, V. M., Toon, G. C., Wunch, D., and Franklin, J. E.: Using high-resolution laboratory and ground-based solar spectra to assess CH4 absorption coefficient calculations, Journal of Quantitative Spectroscopy and Radiative Transfer, 190, 48–59, https://doi.org/10.1016/j.jqsrt.2016.12.013, 2017.

Ngo, N. H., Lisak, D., Tran, H., and Hartmann, J. M.: An isolated line-shape model to go beyond the Voigt profile in spectroscopic databases and radiative transfer codes, Journal of Quantitative Spectroscopy and Radiative Transfer, 129, 89–100, https://doi.org/10.1016/j.jqsrt.2013.05.034, 2013.

Nikitin, A., Lyulin, O., Mikhailenko, S., Perevalov, V., Filippov, N., Grigoriev, I., Morino, I., Yoshida, Y., and Matsunaga, T.: GOSAT-2014 methane spectral line list, Journal of Quantitative Spectroscopy and Radiative Transfer, 154, 63–71, https://doi.org/10.1016/J.JQSRT.2014.12.003, 2015.

Nikitin, A., Chizhmakova, I., Rey, M., Tashkun, S., Kassi, S., Mondelain, D., Campargue, A., and Tyuterev, V.: Analysis of the absorption spectrum of 12CH4 in the region 5855–6250 cm-1 of the $2\nu 3$ band, Journal of Quantitative Spectroscopy and Radiative Transfer, 203, 341–348, https://doi.org/10.1016/J.JQSRT.2017.05.014, 2017.

Nisbet, E. G., Dlugokencky, E. J., Manning, M. R., Lowry, D., Fisher, R. E., France, J. L., Michel, S. E., Miller, J. B., White, J. W. C., Vaughn, B., Bousquet, P., Pyle, J. A., Warwick, N. J., Cain, M., Brownlow, R., Zazzeri, G., Lanoisellé, M., Manning, A. C., Gloor, E., Worthy, D. E. J., Brunke, E.-G., Labuschagne, C., Wolff, E. W., and Ganesan, A. L.: Rising atmospheric methane: 2007-2014 growth and isotopic shift, Global Biogeochemical Cycles, 30, 1356–1370, https://doi.org/10.1002/2016GB005406, 2016.

Parker, R. J., Boesch, H., Byckling, K., Webb, A. J., Palmer, P. I., Feng, L., Bergamaschi, P., Chevallier, F., Notholt, J., Deutscher, N., Warneke, T., Hase, F., Sussmann, R., Kawakami, S., Kivi, R., Griffith, D. W. T., and Velazco, V.: Assessing 5 years of GOSAT Proxy XCH 4 data and associated uncertainties, Atmos. Meas. Tech, 8, 4785–4801, https://doi.org/10.5194/amt-8-4785-2015, 2015.

Rahpoe, N., Von Savigny, C., Weber, M., Rozanov, A. V., Bovensmann, H., and Burrows, J. P.: Atmospheric Measurement Techniques Error budget analysis of SCIAMACHY limb ozone profile retrievals using the SCIATRAN model, Atmos. Meas. Tech, 6, 2825–2837, https://doi.org/10.5194/amt-6-2825-2013, 2013.

Rella, C. W., Hoffnagle, J., He, Y., and Tajima, S.: Local-and regional-scale measurements of CH 4 , δ 13 CH 4 , and C 2 H 6 in the Uintah Basin using a mobile stable isotope analyzer, Atmos. Meas. Tech, 8, 4539–4559, https://doi.org/10.5194/amt-8-4539-2015, 2015.

Rigby, M., Montzka, S. A., Prinn, R. G., White, J. W. C., Young, D., O'Doherty, S., Lunt, M. F., Ganesan, A. L., Manning, A. J., Simmonds, P. G., Salameh, P. K., Harth, C. M., Mühle, J., Weiss, R. F., Fraser, P. J., Steele, L. P., Krummel, P. B., McCulloch, A., and Park, S.: Role of atmospheric oxidation in recent methane growth., Proceedings of the National Academy of Sciences of the United States of America, 114, 5373–5377, https://doi.org/10.1073/pnas.1616426114, 2017.

Röckmann, T., Brass, M., Borchers, R., and Engel, A.: The isotopic composition of methane in the stratosphere: High-altitude balloon sample measurements, Atmospheric Chemistry and Physics, 11, 13 287–13 304, https://doi.org/10.5194/acp-11-13287-2011, 2011.

Rodgers, C. D.: Inverse Methods for Atmospheric Sounding - Theory and Practice, vol. 2, World Scientific, https://doi.org/10.1142/9789812813718, 2000.

Saunois, M., Stavert, A. R., Poulter, B., Bousquet, P., Canadell, J. G., Jackson, R. B., Raymond, P. A., Dlugokencky, E. J., Houweling, S., Patra, P. K., Ciais, P., Arora, V. K., Bastviken, D., Bergamaschi, P., Blake, D. R., Brailsford, G., Bruhwiler, L., Carlson, K. M., Carrol, M., Castaldi, S., Chandra, N., Crevoisier, C., Crill, P. M., Covey, K., Curry, C. L., Etiope, G., Frankenberg, C., Gedney, N., Hegglin, M. I., Höglund-Isakson, L., Hugelius, G., Ishizawa, M., Ito, A., Janssens-Maenhout, G., Jensen, K. M., Joos, F., Kleinen, T., Krummel, P. B., Langenfelds, R. L., Laruelle, G. G., Liu, L., Machida, T., Maksyutov, S., McDonald, K. C., McNorton, J., Miller, P. A., Melton, J. R., Morino, I., Müller, J., Murgia-Flores, F., Naik, V., Niwa, Y., Noce, S., O'Doherty, S., Parker, R. J., Peng, C., Peng, S., Peters, G. P., Prigent, C., Prinn, R., Ramonet, M., Regnier, P., Riley, W. J., Rosentreter, J. A., Segers, A., Simpson, I. J., Shi, H., Smith, S. J., Steele, P. L., Thornton, B. F., Tian, H., Tohjima, Y., Tubiello, F. N., Tsuruta, A., Viovy, N., Voulgarakis, A., Weber, T. S., van Weele, M., van der Werf, G. R., Weiss, R. F., Worthy, D., Wunch, D., Yin, Y., Yoshida, Y., Zhang, W., Zhang, Z., Zhao, Y., Zheng, B., Zhu, Q., Zhu, Q., and Zhuang, Q.: The Global Methane Budget 2000-2017, Earth System Science Data Discussions, pp. 1–138, https://doi.org/10.5194/essd-2019-128, 2019.

Schneising, O., Buchwitz, M., Reuter, M., Bovensmann, H., Burrows, J. P., Borsdorff, T., Deutscher, N. M., Feist, D. G., Griffith, D. W. T., Hase, F., Hermans, C., Iraci, L. T., Kivi, R., Landgraf, J., Morino, I., Notholt, J., Petri, C., Pollard, D. F., Roche, S., Shiomi, K., Strong, K., Sussmann, R., Velazco, V. A., Warneke, T., and Wunch, D.: A scientific algorithm to simultaneously retrieve carbon monoxide and methane from TROPOMI onboard Sentinel-5 Precursor, Atmospheric Measurement Techniques Discussions, pp. 1–44, https://doi.org/10.5194/amt-2019-243, 2019.

Sherwood, O., Schwietzke, S., Arling, V., and Etiope, G.: Global Inventory of Fossil and Non-fossil Methane δ13C Source Signature Measurements for Improved Atmospheric Modeling, https://doi.org/10.15138/G37P4D, 2016.

TCCON: Using the cc option in GGG2014 - Tccon-wiki, https://tccon-wiki.caltech.edu/index.php?title=Software/GGG/Download/GGG{_}2014{_}Release{_}Notes/Using{_}the{_}cc{_}option{_}in{_}GGG2014{&}highlight=continuum+curvature, 2020.

Toon, G. C.: Atmospheric Line List for the 2014 TCCON Data Release, https://doi.org/10.14291/tccon.ggg2014.atm.R0/1221656, 2015.

Tran, H., Ngo, N., and Hartmann, J.-M.: Efficient computation of some speed-dependent isolated line profiles, Journal of Quantitative Spectroscopy and Radiative Transfer, 129, 199–203, https://doi.org/10.1016/J.JQSRT.2013.06.015, 2013.

Veefkind, J. P., Aben, I., McMullan, K., Förster, H., de Vries, J., Otter, G., Claas, J., Eskes, H. J., de Haan, J. F., Kleipool, Q., van Weele, M., Hasekamp, O., Hoogeveen, R., Landgraf, J., Snel, R., Tol, P., Ingmann, P., Voors, R., Kruizinga, B., Vink, R., Visser, H., and Levelt, P. F.: TROPOMI on the ESA Sentinel-5 Precursor: A GMES mission for global observations of the atmospheric composition for climate, air quality and ozone layer applications, Remote Sensing of Environment, 120, 70–83, https://doi.org/10.1016/j.rse.2011.09.027, 2012.

Weidmann, D., Hoffmann, A., Macleod, N., Middleton, K., Kurtz, J., Barraclough, S., and Griffin, D.: The Methane Isotopologues by Solar Occultation (MISO) Nanosatellite Mission: Spectral Channel Optimization and Early Performance Analysis, Remote Sensing, 9, 1073, https://doi.org/10.3390/rs9101073, 2017.

Wunch, D., Toon, G. C., Wennberg, P. O., Wofsy, S. C., Stephens, B. B., Fischer, M. L., Uchino, O., Abshire, J. B., Bernath, P., Biraud, S. C., Blavier, J.-F. L., Boone, C., Bowman, K. P., Browell, E. V., Campos, T., Connor, B. J., Daube, B. C., Deutscher, N. M., Diao, M., Elkins, J. W., Gerbig, C., Gottlieb, E., Griffith, D. W. T., and Hurst, D. F.: Calibration of the Total Carbon Column Observing Network using aircraft profile data, Atmos. Meas. Tech, 3, 1351–1362, https://doi.org/10.5194/amt-3-1351-2010, 2010.

Wunch, D., Toon, G. C., Blavier, J.-F. L., Washenfelder, R. A., Notholt, J., Connor, B. J., Griffith, D. W. T., Sherlock, V., and Wennberg, P. O.: The Total Carbon Column Observing Network, Phil. Trans. R. Soc. A, 369, 2087–2112, https://doi.org/10.1098/rsta.2010.0240, 2011.

Wunch, D., Toon, G., Sherlock, V., Deutscher, N., Liu, C., Feist, D., and Wennberg, P.: The Total Carbon Column Observing Network's GGG2014 Data Version, Tech. rep., https://doi.org/10.14291/tccon.ggg2014.documentation.R0/1221662, 2015.

Yoshida, Y., Ota, Y., Eguchi, N., Kikuchi, N., Nobuta, K., Tran, H., Morino, I., and Yokota, T.: Retrieval algorithm for CO 2 and CH 4 column abundances from short-wavelength infrared spectral observations by the Greenhouse gases observing satellite, Atmos. Meas. Tech, 4, 717–734, https://doi.org/10.5194/amt-4-717-2011, 2011.

Yoshida, Y., Kikuchi, N., Morino, I., Uchino, O., Oshchepkov, S., Bril, A., Saeki, T., Schutgens, N., Toon, G. C., Wunch, D., Roehl, C. M., Wennberg, P. O., Griffith, D. W. T., Deutscher, N. M., Warneke, T., Notholt, J., Robinson, J., Sherlock, V., Connor, B., Rettinger, M., Sussmann, R., Ahonen, P., Heikkinen, P., Kyrö, E., Mendonca, J., Strong, K., Hase, F., Dohe, S., and Yokota, T.: Improvement of the retrieval algorithm for GOSAT SWIR XCO2 and XCH4 and their validation using TCCON data, Atmospheric Measurement Techniques, 6, 1533–1547, https://doi.org/10.5194/amt-6-1533-2013, 2013.

Zhou, M., Langerock, B., Sha, M. K., Kumps, N., Hermans, C., Petri, C., Warneke, T., Chen, H., Metzger, J. M., Kivi, R., Heikkinen, P., Ramonet, M., and De Mazière, M.: Retrieval of atmospheric CH4 vertical information from ground-based FTS near-infrared spectra, Atmospheric Measurement Techniques, 12, 6125–6141, https://doi.org/10.5194/amt-12-6125-2019, 2019.